Joule

CellPress REVIEWS

Review

Uncharted Waters: Super-Concentrated Electrolytes

Oleg Borodin,[1,2,*] Julian Self,[3,4] Kristin A. Persson,[3,4,*] Chunsheng Wang,[5,*] and Kang Xu[1,2,*]

As a legacy left behind by classical analytical electrochemistry in pursuit of ideal electrodics, and classical physical electrochemistry in pursuit of the most conductive ionics, the study of non-aqueous electrolytes has been historically confined within a narrow concentration regime around 1 molarity (M). This confinement was breached in recent years when unusual properties were found to arise from the excessive salt presence, which often bring benefits to electrochemical, thermal, transport, interfacial, and interphasial properties that are of significant interest to the electrochemical energy storage community. This article provides an overview on this newly discovered and under-explored realm, with emphasis placed on their applications in rechargeable batteries.

HISTORY OF THE ART: LEGACY AND DEVIATION

Since the dawn of electrochemistry, high salt concentration in electrolytes has never been favored. While the analytic school of electrochemistry focused on producing accurate mathematic descriptions of electrodic behaviors in the ideal state free of interionic interferences,[1,2] a requirement that can only be met when the ions under investigation be kept at infinitesimal, the physical school of electrochemistry pursued the practical application of electrochemical devices, where the optimum ionic transport is of primary importance.[3–5] The "1 molarity (M) legacy" of non-aqueous electrolytes originated from such pursuits, because the maxima of ionic conductivities almost always occur near the salt concentration of 1.0 M for all systems. These maxima are the results of compromise between two major contributors to transport properties: (1) ionic carrier number (n) proportional to the salt dissolution and dissociation and (2) ionic mobility (μ) associated with the matrix viscosity (η) of electrolyte (Figure 1). Such relation holds true for systems where the movement of an ion is highly coupled with its surroundings (i.e., solvent molecules) via the solvation sheath. The most extreme case is perhaps the solid-polymer-electrolytes, which can be viewed as macromolecular version of non-aqueous electrolytes.[6] In those highly coupled electrolyte systems, the ionic transport cannot happen without the cooperative movement of polymeric segments that solvate the ions. It was the belief that the above ion-solvent coupling would keep intensifying with increasing salt concentration that had discouraged interest in exploring the super-concentration realms.

The beneficial aspects of the saturated electrolytes were noticed as far back as 1985 by McKinnon and Dahn, who reported that a saturated propylene carbonate (PC) solution of $LiAsF_6$ demonstrated unusual electrochemical intercalation behavior toward a layered host that could not be possible in *1M* electrolyte.[7] However, the earliest serious attempt to breach the concentration confinement ironically happened with polymer electrolytes. In order to free Li^+-movement from the traps formed by its polymeric solvation cages, Angell et al. ventured into the "uncharted waters" of super-concentration (Figure 2).[8] The "polymer-in-salt" concept proposed

Context & Scale

The traditional efforts in electrolytes have been mostly evolving around the "1 M" region, where maximum ion conductivities occur in the majority of non-aqueous electrolyte systems. However, recent deviation from this "optimum" concentration has revealed to us that there is a new world. In the super-concentrated regions, the reversed salt/solvent ratio brought dramatic changes in bulk liquid structures, ion transport, and interfacial and interphasial properties. Some of these unusual properties have been found to introduce benefits to electrochemical, thermal, transport, interfacial, and interphasial properties that are of significant interest to the electrochemical energy storage community. This article provides a comprehensive overview on this newly discovered and under-explored realm.

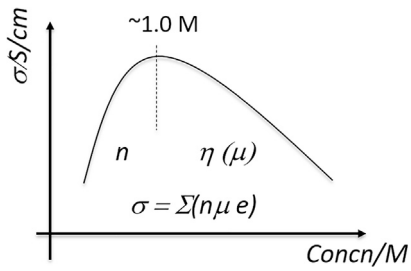

Figure 1. Legacy of 1 M
The compromise between ionic carrier number (*n*), ionic mobility (μ) and solution viscosity (η) creates the maxima in ionic conductivities, which occurs in the neighborhood of 1.0 m for most non-aqueous electrolytes.

involved polymers being added as minority to the bulk molten salt or a salt mixture in order to lower the melting point, in the hope that the polymer as mechanic skeleton would impart its rubbery characteristic while the salt maintains most of the ionic movement without negative effects from polymeric traps. Although "polymer-in-salt" concept eventually encountered the practical difficulty of finding room-temperature molten salts with an electrochemical stability window wide enough to support meaningful battery chemistries, it did reveal that unexpected benefits might arise beyond and away from the narrow confinement of diluted salt concentration. Similar concept now is being actively explored in the development of the polymer-electrolyte-in-ceramic hybrid electrolytes with the interfacial region being the key to optimizing the overall ionic transport.[9,10]

A decade later, unusual interphasial properties were noticed with a similar venture in liquid non-aqueous electrolyte. According to Jeong et al.,[11] the well-known exfoliation of graphite by PC would not happen when some lithium salts are used at a higher-than-usual concentration. However, the general enthusiasm in super-concentrated electrolytes was not initiated until another decade later, when Watanabe and

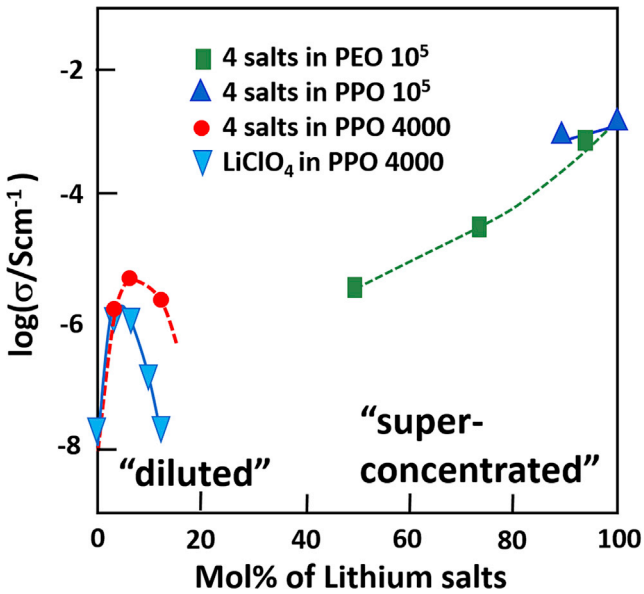

Figure 2. An Early Attempt to Depart from the "1 M Legacy"
Polymer-in-Salt" approach breaches the concentration confinement imposed by *n*-η compromise. "4 salts" refers to the mixture of lithium iodide, lithium chlorate, lithium perchlorate, and lithium nitrate, while PEO and PPO represent poly(ethylene oxide) and poly(propylene oxide), respectively, followed by numbers indicating their molecular weights. Here the polymers serve as the macromolecular solvents for lithium salts. Graph reconstructed from part of data reported in Angell et al.[8]

[1]Joint Center for Energy Storage Research, U.S. Army Research Laboratory, Adelphi, MD 20783, USA

[2]Battery Science Branch, Sensors and Electron Devices Directorate, U.S. Army Combat Capabilities Development Command, Adelphi, MD 20783, USA

[3]Energy Technologies Area, Lawrence Berkeley National Laboratory, Berkeley, CA 94720, USA

[4]Department of Materials Science and Engineering, University of California, Berkeley, CA 94720, USA

[5]Department of Chemical and Biomolecular Engineering, University of Maryland, College Park, MD 20742, USA

*Correspondence:
oleg.a.borodin.civ@mail.mil (O.B.),
kapersson@lbl.gov (K.A.P.),
cswang@umd.edu (C.W.),
conrad.k.xu.civ@mail.mil (K.X.)

https://doi.org/10.1016/j.joule.2019.12.007

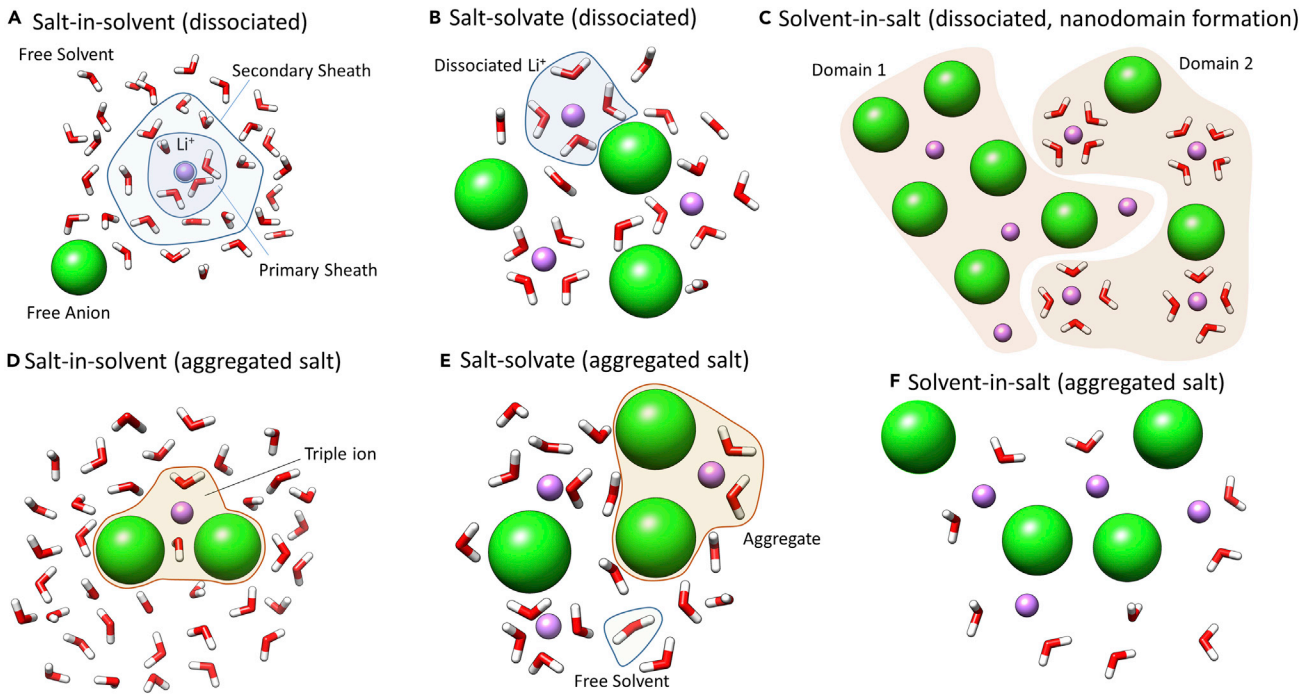

Figure 3. From "Dilute" to "Super-Concentrated" Regime

Schematic representation of three salt concentration regimes for the dissociating (A–C) and aggregating (D–F) salts: (A and D) ion solvation sheath in "diluted" electrolytes with the three layers: the primary and the secondary solvation sheaths and the bulk free solvent, while the anion remains little solvated (green); and (B, C, E, and F) the solvation structure in a super-concentrated electrolyte, where the primary solvation sheath is disrupted by the insufficiency of solvent molecules and the presence of anions in the close vicinity of central cation. The shared solvent molecules constitute various interpenetrated solvation sheaths.

co-workers described a series of unusual properties from the glyme-based super-concentrated electrolytes.[12–16]

STATE OF THE ART: SUPER-CONCENTRATION AND ITS DERIVATIVES

Considered a transition regime between the conventional "1 M" electrolytes and neat ionic liquids or molten salts, the so-called "super-concentrated electrolytes" do not have a clear and quantitative definition. Depending on the nature of the solvents and the corresponding capability of dissolving salts, the salt concentration involved ranges from 3∼5 M in non-aqueous media up to 4∼10 M in aqueous media. At these high salt concentrations, significant ion–pairing and aggregation occurs, while limited solvent molecules therein are largely bound to cations, leading to entirely new structures at both molecular and long-range scales that affects a host of properties covering transport, thermal, mechanical, electrochemical, interfacial, and interphasial.

Instead of defining a finite concentration limit, we can tentatively classify all electrolytes into three distinct regimes by looking at how ion solvation sheath is structured, as shown in Figure 3: (1) "salt-in-solvent" electrolytes, where the population of solvent molecules is higher than needed to complete the primary solvation sheath for the cations; (2) "salt-solvate" electrolytes, where the population of solvent molecules is just sufficient to complete the primary solvation sheath for the cations, so that stoichiometric solvates often form for the largely dissociating salts; (3)

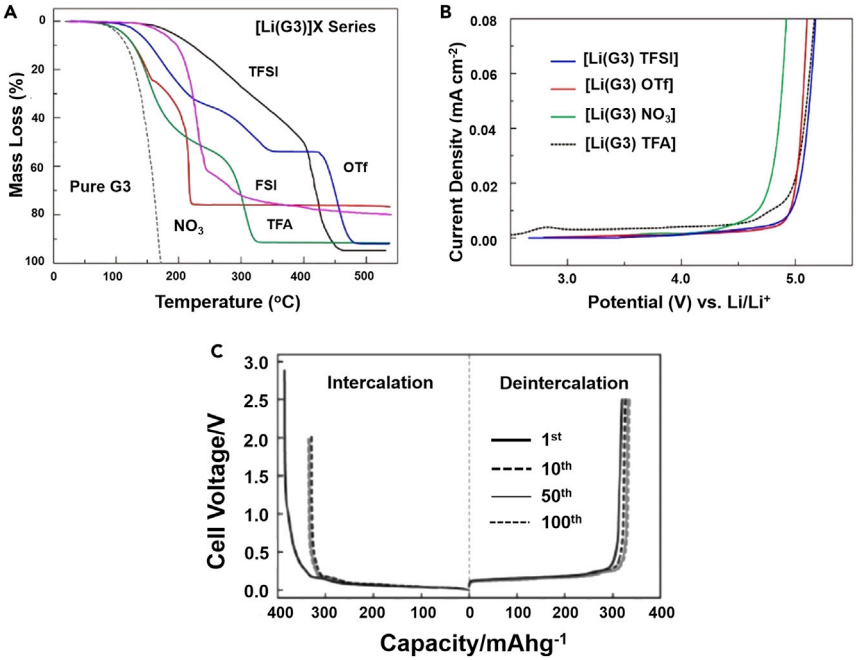

Figure 4. The Novelties of Super-Concentration

Unusual thermal, transport, and interfacial properties found in super-concentrated lithium electrolytes based on multi-glyme Solvents.[12,15]

(A) Thermogravimetric analysis of LiX(G3) solvent solvates.[12]

(B) Linear sweep voltammograms of [Li(G3)]X at scan rate 1 mV s^{-1} at 30°C at Pt working electrolyte and using Li metal as a counter and Ueno et al.[12];

(C) The charge-discharge profiles of the [graphite electrode | TG-LiFSI electrolyte | lithium metal] cell in the 1st, 10th, 50th, and 100th cycles.[12,19] Reprinted with permission from[12,15] Copyright 2011, 2012 American Chemical Society.

"solvent-in-salt" electrolytes, where the primary solvation sheath for the cation cannot be completed due to insufficient solvent population.

While the conventional electrolytes at ~1.0 M belongs to "salt-in-solvent" category, super-concentrated electrolytes are covered by the latter two categories, with the "salt-solvates" also often referred to as "quasi-ionic liquids" or "solvated ionic liquids" in order to highlight their similarity to room-temperature ionic liquids (RTILs) due to low fraction of "free" solvent. The primary limiting condition on whether a super-concentrated electrolyte exists or not is apparently the solubility of a salt in a given solvent that is related to the melting point of solvates, disorder, and crystallization kinetics that can give rise the crystallinity and gaps at high salt concentration.[17,18] While the high donicity of ether molecules makes them the popular choices, the weakly associated anions such as bis(trifluoromethanesulfonyl)imide (TFSI) can ensure maximum ion dissociation. Using ether molecules of varying length such as triglyme (G3) or tetraglyme (G4), Watanabe and coworkers demonstrated that the tight binding of all glyme molecules by high ionic populations induced a series of dramatic properties that are otherwise impossible at dilute salt concentrations,[12–16,19] the most representative of which include the thermal stability up to 200°C (Figure 4A) and altered electrochemical behaviors on both cathode and anodes, as evidenced by the resistance against oxidation on Pt surface (Figure 4B) as well as $LiCoO_2$ when charged to 4.2 V,[13] and ability to support reversible Li^+-intercalation chemistry with graphitic anode without the co-intercalation behavior typically associated with ethers (Figure 4C). They attributed the emergence of these

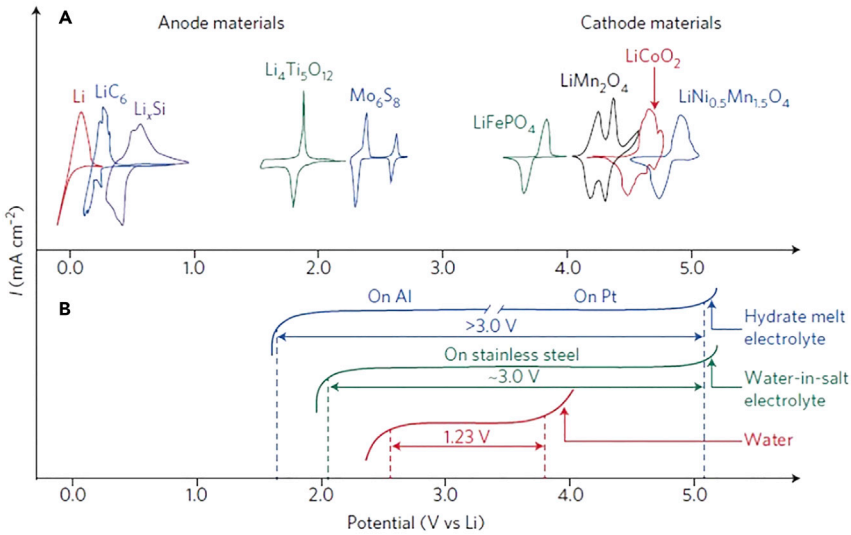

Figure 5. New Frontiers of Waters

Expanded electrochemical stability windows of aqueous electrolytes via super-concentration

(A) The redox potentials of major anode and cathode materials: Li-metal, Mo_6S_8, $Li_4Ti_5O_{12}$, $LiMn_2O_4$, $LiFePO_4$, $LiCoO_2$, and $LiNi_{0.5}Mn_{1.5}O_4$;

(B) Redox reactions of water molecules at pH = 7 evolves hydrogen and oxygen at anode and cathode surfaces, respectively, giving rise to a thermodynamic stability window of 1.23 V, whereas super-concentration (21 mol kg^{-1} LiTFSI in WiSE, and 27.8 mol kg^{-1} LiTFSI+LiBETI in the hydrate melt electrolytes) significantly expands windows to larger than 3.0 V. Reprinted with permission from Xu and Wang.[33] Copyright 2016 Springer Nature.

unusual properties to the solvation of high population of Li^+ by limited population of solvent (glyme) molecules, resulting in elimination of "free" solvent.

Among the numerous candidates as potential solvents and salts to make an electrolyte super-concentrated, two classes of compounds have been receiving special favors due to their unique properties: *ethereal solvents* for their strong dissolution and chelating capabilities toward cations and *imide-based salts* (LiTFSI, or its homologs such as lithium bis(pentafluoroethanesulfonyl)imide, LiBETI, or lithium bis(fluorosulfonyl)imide, LiFSI) for their extra-ordinary tendency to dissolve and dissociate in almost all polar solvents. Most of the successful super-concentrated electrolytes rely on at least one of these components, with the successful examples include the "solvent-in-salt" electrolytes of Suo et al. based on LiTFSI dissolved in 1,2-dimethoxyethane (DME) and 1,3-dioxolane (DOL) at concentrations up to 7 M,[20] the "super-concentrated" electrolytes of Yamada et al.[21] based on either LiTFSI dissolved in acetonitrile up to 4 M or LiFSI dissolved in dimethyl carbonate up to 10 m,[22] or the "self-extinguishing electrolytes" of Shiga et al.[23] based on NaFSI or LiFSI dissolved in phosphate esters or amides up to 3 M.

Perhaps the most extreme scenario of super-concentrated electrolytes are the so-called "water-in-salt" electrolyte (WiSE) by Suo et al. based on LiTFSI dissolved in water at concentrations up to 21 m (or ≈5 M)[24] and the many variations including sodium and zinc electrolyte,[25–30] which have brought unprecedented electrochemical stabilities to aqueous electrolytes and enabled revolutionary aqueous battery chemistries that were otherwise impossible (Figure 5).[31–33]

To minimize the high cost disadvantage induced by high salt concentration, there have been numerous efforts toward reducing the salt usage without compromising

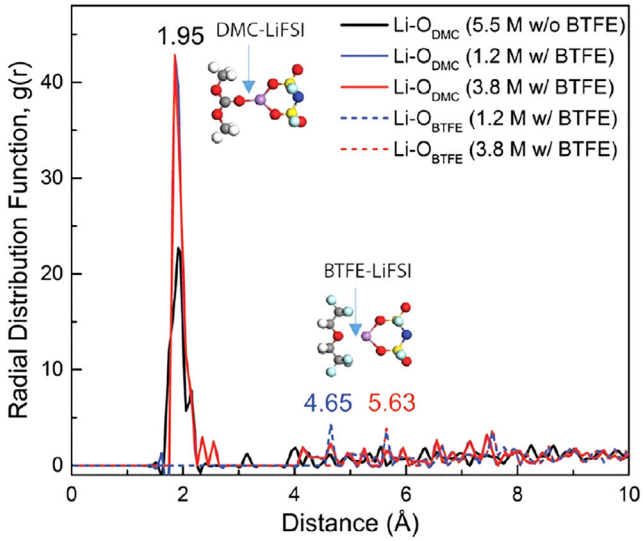

Figure 6. Localizing Super-Concentration by Non-solvent: The Electrolyte

(A) Radial distribution functions of Li–O_{DMC} and Li–O_{BTFE} pairs calculated from the last 5 of 15 ps AIMD simulation trajectories at 30°C in electrolyte consisting of LiFSI dissolved in mixture of DMC and a fluorinated ether (BTFE). Insets shows the structures of DMC–LiFSI and BTFE–LiFSI solvent-salt pairs. Due to much shorter AIMD run length (15 ps) compared to the average time it takes a Li^+ to renew its solvation shell in similar electrolytes (~10^2 ps)[42] the resulting solvate structure was "quasi-equilibrated".[34] Reprinted with permission from Chen et al.[34] Copyright WILEY-VCH 2018.

the advantages brought by super-concentration, such as preferred ion transport, non-flammability, and interfacial and interphasial stabilities. One innovative approach is the so-called "localized high concentration electrolytes," where a Li^+ non-coordinating co-solvent (usually a polyfluorinated ether) was used to dilute the parental electrolyte, so that the overall salt concentration in electrolyte would rest in the more conventional range near 1.0 M rather than super-concentration (Figure 6).[34–38] The essence of such strategy is to separate the bulk and interfacial responsibilities of an electrolyte and assign these roles to varying phases that are microscopically separated. In all the electrolyte compositions reported, such role-separation leverages the poor solvation of Li^+ or Na^+ by various fluorinated molecules. Thus, while the immediate local environment of cations (Li^+ or Na^+) still maintains the solvation structure of super-concentrated electrolytes, which is often responsible for the interphasial chemistries at electrode surfaces, the bulk properties (ion transport, viscosity, or wettability toward the electrodes and separators) were mainly defined by the average composition of the bulk electrolyte that still bear the nature of diluted regime. The simultaneous stabilization of the lithium metal and the high capacity and high voltage cathodes might have benefited from the highly fluorinated CEI formed by the partially fluorinated non-solvent and the defluorination of both LiFSI and $LiPF_6$,[39–41] while most of the "oxidatively weak" but highly Li^+-solvating solvents were kept away due to the coulombic repulsion at the cathode surface. Because the strong salt aggregation is preserved locally in the electrolyte as a non-coordinated diluent is added, the preferential salt reduction that requires such aggregation is also preserved in the diluted regime.[28,41] From this prospective, the electrolyte based on mixture of coordinating and fluorinated non-coordinating co-solvent also fits the framework of the "localized high concentration electrolytes" if the fraction of the non-coordinated co-solvent is sufficiently high.[28]

In several cases, exotic solvent systems traditionally thought impossible have also been used, such as ether or alkylphosphate esters, achieving both bulk and interfacial benefits, in addition to the cost reduction because of the lower apparent salt concentration. To some degree this design principle is a logical extension of the original design of the lithium ion battery electrolytes comprised from the mixtures of ethylene carbonate (EC) and dimethyl carbonate (DMC), where EC role was to stabilize graphite anode and dissociate salt, while DMC or other cycle carbonate reduced electrolyte viscosity and lowered its melting point.[43] As the mechanism and dynamics of this class of electrolytes become better understood, there should be plenty of new solvent-salt combinations to emerge.

SOLVATION AND LIQUID STRUCTURE

Electrolyte is responsible for providing electric current between cathode (positive) and anode (negative), and such current that be solely carried by moving ions. With the rare exceptions of salts in molten (ionic liquid) or decoupled ceramic or glassy states, a majority of these mobile ions come from the dissociation of salts by polar solvent molecules.[43] The resultant solvated ions constitute the actual ionic species that are mobile in electrolytes. Apparently how these ions interact with solvent molecules and among themselves define a series of parameters of the resultant electrolytes, ranging from mechanical (compressibility, viscosity), thermal (heat conductivity and capacity), to chemical (solubility, activity, reactivity), transport, and electrochemical (interfacial and interphasial). Most of these properties are key in dictating the performance of any electrochemical devices.

The classical Debye-Hückel model assumes complete dissociation of salt while ignoring direct solvent-salt interactions beyond providing mean-field like screening through permittivity, while modern ionics recognizes the vital importance of polar solvent molecules in stabilizing the ions in dissociated form.[3] Bernal and Fowler were the pioneers who quantified how the introduction of an ion into bulk solvent induces the neighboring solvent molecules to reorient their dipoles around this ion, thus breaking the structure of the bulk solvent.[44] A "three layer" model was proposed (Figure 3A), in which the most immediate solvent molecules forms the strongest association with the ion and would likely to remain with the ion during its translational movement, while the solvent molecules far away from the ion maintain the undisturbed bulk structure. Somewhere between these two regions is an intermediate layer, whose bulk structure is broken by the coulombic field of the ion but their distance is not close enough to associate themselves with the moving ion. Nowadays we referred this inner and intermediate solvation layers as "primary" and "secondary" solvation sheaths, respectively. Such model actually assumes that sufficient solvent molecules are available for the ions to recruit, which does not hold true in super-concentration regimes due to the high salt/solvent ratios. The insufficiency of solvent molecules would lead to the disappearance of the bulk and secondary solvation sheaths, while the solvent molecules are forced to be shared by different ions. At extreme scenarios the anion-cation distance are so compressed that they enter the primary solvation sheaths of each other (Figures 3C–3F). Such disruption of classical solvation sheath not only alters the local solvation environment around the ions, but also introduces liquid structures in long-range due to the aggregation of ions (Figures 3C–3F).

Cation Solvation and Salt Dissociation

It is well established that better salt dissociation occurs with the stronger solvent-salt interaction and weaker cation-anion interaction. Ideal salt dissociation leads to free

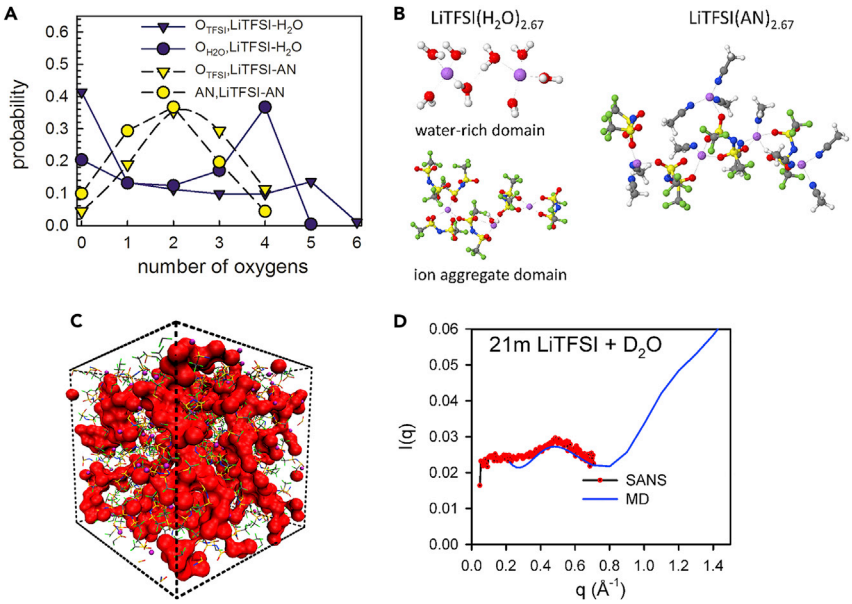

Figure 7. New Liquid Structures at Super-Concentrations

(A) A distribution of solvent and oxygen of TFSI around Li^+ (<2.8 Å) in H_2O/LiTFSI = 2.67 (4.94 mol L^{-1}, 20.8 mol $kg_{solvent}^{-1}$) (shown in dark blue) and AN/LiTFSI=2.67 (3.6 mol L^{-1}, 9.14 mol $kg_{solvent}^{-1}$) (shown in yellow). Probability for a Li^+ to have zero number of O_{TFSI} corresponds to the solvent separated cations.[49]

(B) The most probable lithium solvates extracted from MD simulations of LiTFSI in H_2O and AN at the solvent/Li = 2.67 salt concentration.

(C) A snapshot of the MD simulation box for 21m LiTFSI in H_2O with water with the $Li^+(H_2O)n$ domain shown as a red isosurface, while the $TFSI^-$ anions shown as ball-stick model.[49]

(D) Structure factor for 21m LiTFSI in D_2O from MD simulations and SANS measurements.[49]

ions with negligible interionic attractions. In reality, an electrolyte of higher fraction of free ions is often obtained in the salt-in-solvent regime, which offers higher conductivity at a given viscosity. However, it is less clear if the same principle could be applied to the solvent-in-salt electrolyte when the population of solvent molecules is insufficient to fully coordinate all cations while separating cations from anions. In fact, it remains a question whether a significant fraction of free ions could exist in the solvent-limited solvent-in-salt regime. When a Li^+ cation can only access half of the solvent molecules needed to complete its first solvation sheath (i.e., solvent/Li = 2), the fraction of free ions was found to be less than 3% for the acetonitrile (AN) solutions of $LiPF_6$, LiFSI, LiTFSI, $LiBF_4$, or $LiClO_4$.[45–47] Generally, in aprotic super-concentrated (3.5–5 M) electrolytes such as LiFSI in DME[48] or LiTFSI in AN,[49] the Li^+-coordination have a similar contribution from solvent and anion (2 solvents and 2 anions), as shown in Figure 7A for LiFSI in AN (AN/Li=2.67). The distribution of AN solvent and oxygen of TFSI around Li^+ is single peaked around two, with the majority of ions existing as ion-aggregates or ion pairs with a very small fraction of free solvent separated Li^+. Therefore, the cation transport has to occur in these solvent-in-salt electrolytes either via the anion and solvent exchange or the charged cluster diffusion due to very small fraction of the solvent separated (or free) Li^+.

Replacing AN with water, which is a much stronger solvent compared to many aprotic solvents familiar to battery researchers, gives rise to a rather different Li^+-solvation sheath composition. At the same solvent/Li ratio of 2.67, a high fraction of the

fully hydrated Li^+ was found in WiSE in MD simulations, despite that the first Li^+ solvation sheath cannot be fully completed due to the insufficient number of water molecules. Thus, in WiSE with 21 m of LiTFSI (H_2O/Li = 2.67), a significant "disproportionation" in Li^+-solvation sheath occurs, leaving a high portion (~40%) of Li^+ exclusively surrounded by water molecules only, while the rest (~40% of Li^+) are mainly surrounded by TFSI (Figures 7A and 7B).[49] The stronger ability of water to solvate both Li^+ and anion compared to AN is responsible for such "disproportionation" in the local Li^+-environments, which in longer length leads to a heterogeneity on nano-scale (~1 nm) with water-rich and anion-rich regions, instead of an "average" solvation environments where solvent (water) and anion evenly distribute (Figure 7C). Such a nano-heterogeneity was experimental proved by small-angle neutron scattering (SANS, Figure 7D), where a peak observed at ~1.0 nm (or at q = 0.45 $Å^{-1}$) should correspond such structure.

Counterintuitively, despite the stronger dissociation of LiTFSI in water than in AN, binding energy of the $Li^+(H_2O)_4$ is smaller than that for the $Li^+(AN)_4$, thus indicating that the anion solvation by water versus AN is important for achieving salt dissociation.[49] The cluster-continuum quantum chemistry calculations of the Li-Anion dissociation predict the lithium salt dissociation in dilute solutions in good agreement with spectroscopic measurements,[50] however, they do not fully take into account the anion-solvation contribution and, therefore, should be used only for the same class of electrolyte with a similar anion solvation in order to provide consistent predictions.

When extending the solvation disproportionation to bivalent cations, an interesting distortion occurs due to the difference in cations' capability to interact with anions and solvent molecules. With 1m $Zn(TFSI)_2$ dissolved as minority salt in WiSE (21 m LiTFSI), the solvation sheath of Zn^{2+} was found to be solely occupied by anions (TFSI) without water presence, while a high fraction of free Li^+ were solely solvated only by water.[28] Apparently, Zn^{2+} loses its competition for water molecules to the majority cation Li^+.[28]

The "salt-solvate" electrolytes systematically studied by Watanabe and co-workers represent an intermediate concentration range, where the population of solvent molecules are just enough to complete the first solvation sheath of Li^+. Glymes of varying length (G*n*, where *n* in CH_3-$[CH_2CH_2O]_n$-OCH_3 shows the number of solvating oxygens) were used,[12–16,19,51] although other solvent molecules could also form salt-solvates, such as AN or carbonate esters studied by Henderson and co-workers.[17,45,46,52] In such systems, the presence of free solvent leads to both thermal and electrochemical instabilities as measured by mass loss at lower temperatures[14,52] (Figure 4A) and degrading oxidative stability (Figure 4B).[12,15] Weaker binding solvents such as THF<G1<G2<G3 (in the order of stronger solvation toward Li^+) also lead to the increased salt aggregation and higher fraction of free solvents in the super-concentration regime, thus degrading the oxidative stability of the salt-solvates.[12,51]

The relative strength of the Li^+ interaction with solvents versus anions in dilute solutions determines the extent of salt dissociation, ion aggregation, and the correlation between cation and anion during ion transport. The later measure of the degree of ion uncorrelated motion was defined as "ionicity" by Watanabe et al., which can be probed via a combination of impedance and NMR techniques or conductivity and viscosity by relating molar conductivity of electrolyte (Λ_{imp}) to that calculated using ion self-diffusion coefficients (Λ_{NMR}) or the "ideal" KCl line based on a 1M KCl

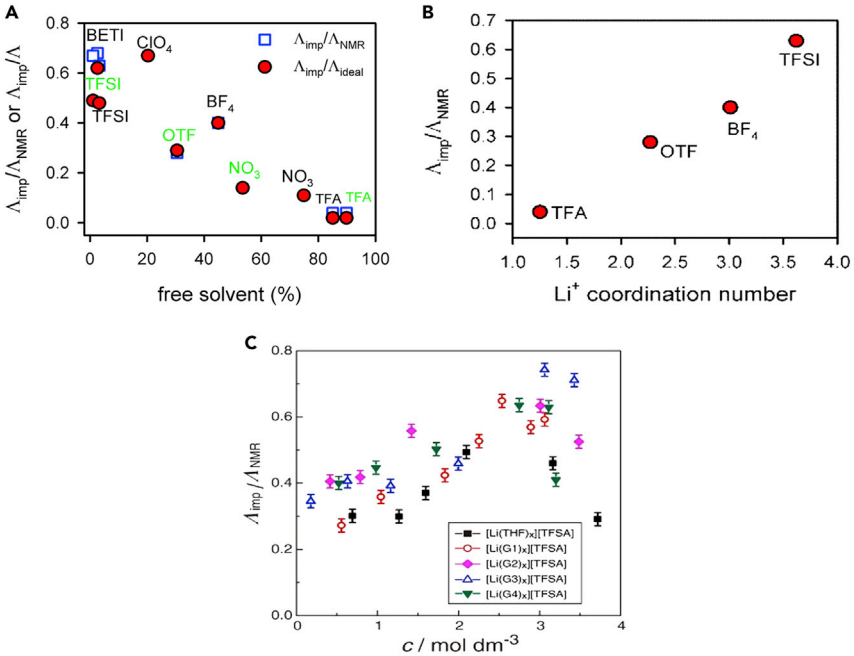

Figure 8. Ion-Solvent Interaction at Super-Concentration

(A) A relation between a fraction of free solvent and degree of uncorrelated ion motion (often called ionicity) for G3(Li)Anion (in green labels) and G4(Li)Anion solvated salts (black labels). Anion abbreviations: $N(SO_2CF_3)_2$ (TFSI), CF_3SO_3 (OTF), $N(SO_2CF_2CF_3)_2$ (BETI), CF_3CO_2 (TFA). Compiled from NMR, conductivity and viscosity data from Ueno et al.[12] and Raman measurements.[56]

(B) The degree of ion uncorrelated motion (iconicity) for Li(G4)[TFSI,BF_4,TFA], Li(G3)ClO_4 solvated salts[12] plotted versus the Li^+ solvation number in EC:LiAnion (EC:Li = 10) extracted from Raman spectroscopy.[57]

(C) Ionicity ($\Lambda_{imp}/\Lambda_{NMR}$) at 30°C for [Li(glyme or THF)$_x$][TFSA] mixtures as a function of concentration.[51] Plotted based on data from[51] Copyright 2014 American Chemical Society.

aqueous solution (Λ_{ideal}). An ideal electrolyte should have an ionicity of 1.0, reflecting no correlation between the cation and anion motion (e.g., $\Lambda_{NMR}=\Lambda_{imp}$). It is realized in the completely dissociated dilute electrolyte, and such ideal behavior can only be reached in good solvents at very low concentrations.[53] If ionic solvation is poor, the opposite behavior (e.g., $\Lambda_{NMR}> \Lambda_{imp}$) is observed with the ion aggregation increasing and the cation-anion motion becoming more correlated as salt concentration decreases.[54]

In the salt-solvate electrolytes there is a strong inverse dependence of the extent of ion uncorrelated motion (ionicity, a dynamic property) and a fraction of free solvent (structural property) as shown in Figure 8A. The lower the fraction of free solvent, the more solvent participates in the Li^+ solvation, dissociating salt and making ionic motion less correlated due to electrostatic screening. The ion correlation and aggregation trends for the glyme-based solvated salts obtained from dynamic and spectroscopic measurements (Figure 8A) are similar to the trends deduced from the previous study of phase behavior and crystalline solvates for $(glyme)_n$-LiX mixtures by Henderson[17]: $LiN(SO_2CF_3)_2$ (TFSI), $LiAsF_6$ < $LiClO_4$, LiI < $LiBF_4$ < $LiCF_3SO_3$ < $LiNO_3$, LiBr < $LiCF_3CO_2$. Similar trends were reported for "ionicity" in 0.75 M γ-Butyrolactone (GBL): $LiPF_6$ ≈ LiTFSI ≈ LiBETI > $LiBF_4$ > LiOTF.[55] There is also a very good correlation between the "ionicity" ($\Lambda_{imp}/\Lambda_{NMR}$) in the glyme salt-solvates and the Li^+ solvation number in the EC-based electrolytes at the lower salt concentration (EC/Li = 10) as shown in Figure 8B, indicating that the similar

trends for salt dissociation and ionic correlation seem to hold for these different solvents (glyme and EC).

While the more associated salts result in lower ionicity (higher correlation of ion motion) and higher fraction of free solvent, the higher ionicity does not necessarily reflect high ion dissociation as salt concentration increases toward the solvated salt regime. Approaching super-concentration, counterintuitively, leads to increased ionicity ($\Lambda_{imp}/\Lambda_{NMR}$) around 3M in Figure 8C, despite increasing ion pairing and aggregation that occur simultaneously.[51] Maximum ionicity is reached at a fixed stoichiometric ratio of ether units and Li^+ (EO/Li^+~4), which happens to be a typical Li^+ solvation sheath structure in ether-based solvents. We attribute it to the anticorrelation of the $Li^+(EO)_4$ solvate and anion motion as required by the conservation of momentum in this highly dissociated electrolyte with little free solvent. Similar high ionicity (0.6–0.8) was found for the highly concentrated WiSE, which is significantly higher than the fraction of the solvent separated Li^+ that is only 0.4.[49]

Anion Solvation

The solvation of anions is highly system-specific. In most commonly used non-aqueous solvents, anions are typically not, or at least very little, solvated as compared with cations.[58] This is owing to the facts that most non-aqueous solvent molecules are better electron donors rather than acceptors, and that anions are much larger than cations, leading to much smaller coulombic interactions with the solvent. Typical anions PF_6^- and FSI^- have been found via liquid secondary ion mass spectra (SIMS) to be much less strongly solvated by either carbonate or ether solvents than their counterion (Li^+),[58,59] where a well-defined solvation sheath no longer exists. However, this cation-preferred solvation behavior would change when the solvent molecules become water, whose bipolar nature has been well established. It is this water-TFSI association that further assists in the LiTFSI salt dissociation leading to the Li^+-solvation shell disproportionation that is directly responsible for the long-range (~1.0 nm) heterogeneity network found in WiSE mentioned above.[49] The question remains unanswered regarding whether such a structure exists in non-aqueous electrolytes at super-concentration regimes, but obviously the weak solvation behavior of anions makes it much more difficult to dissociate lithium salt as needed to form the solvent-rich and salt-rich nano-domains.

ION TRANSPORT

In the classical Bernal-Fowler model, the solvent molecules in a primary solvation sheath are considered "permanently" attached to the ion, hence the sheath composition should remain static during the ionic movement.[44] While these solvent molecules indeed have stronger binding with the ions than the molecules in secondary and bulk regions, the stability of the sheath structure is only true in the time scale of pico- to nano-seconds, as evidenced by the fact that these different solvent molecules can only be differentiated using ultra-fast spectroscopy. Furthermore, MD simulations indicate that residence time of Li^+ with solvent molecules could be longer or shorter than the Li^+-anion residence times depending on the salt, solvent, and concentration.[60–62] Hence, with the exception of dilute electrolytes based on a good solvent or aqueous electrolytes, one can almost never rely exclusively on the free cations (fully solvent separated from anions) to achieve high ionic conductivity. Even one of the most dissociating salts such as LiTFSI in dilute regime (solvent/Li = 20) show the degree of uncorrelated motion ("ionicity") between 0.1 and 0.64 for 14 solvents of interest to batteries, which is significantly below 1 for the fully dissociated and uncorrelated system.[63]

Vehicular versus Structural Ion Motions

The manner of ionic transport across the electrolytes can be described as either vehicular or structural. In the former, the solvation sheath travels with the solvated ion, while in the latter, the ion hops via a serial ion association-dissociation process if the solvating sites are immobilized (as in solid state electrolytes), or via frequent exchange of solvent molecules (when these solvent molecules are mobile themselves).[60–62,64,65] Of course, these scenarios represent two extremities. An ion could travel simultaneously in both manners, because, given the transient stability of solvation sheath, ions would eventually experience complete replacement of the inner solvent members in their primary solvation sheath.

The relative contributions of the vehicular and structural (solvent or anion exchange) modes to the cation diffusion can be quantified via a ratio of the averaged distance a solvent (or anion) moves together with a cation to the size of the solvent (or anion). When a cation moves multiple solvent sizes before it exchanges the solvent molecules in its coordination shell, the transport mechanism is largely vehicular as observed for the Li^+ in glymes and aqueous electrolytes in both solvent-in-salt and solvated-salts-regimes if the salt is strongly dissociated such as LiTFSI.[49,60,66] The strong chelation of Li^+ by multiple ether oxygens make the Li^+-transport in ether-based electrolytes almost exclusively vehicular, as Li^+ moves around three solvent sizes before it exchanges all solvent molecules for 1,2-dimethoxyl ethane (DME) and pentaglyme (G5, denoted as EO_6 in Figure 9A).[60] Hence, a Li^+-glyme complex largely travels in its entirety without disruption of the solvation sheath. Such inference was supported by experimental observation that the diffusion constant ratio $D_{solvent}/D_{Li^+}$ approaches 1.0 in glyme-based electrolytes as concentration approaches the solvated salt regime.[51,67] When an oligoether chain length increases past the 5–6 repeat units needed to solvate a single Li^+ to 54 repeat units, the Li^+-transport mode becomes more structural, as represented by Li^+ moving along the polymer chain and hopping between the polymer segments (Figure 9A) in addition to the motion with the polymer segment. The weaker Na^+-glyme binding as compared to Li^+-glyme and the larger size of the Na^+-solvation sheath result in a switch of the transport mechanism from being primarily vehicular to structural with frequent solvent exchanges for DME doped with NaFSI and NaTFSI.[66,68] A similar trend was observed in the ionic liquid-based electrolytes, where a dominance of the vehicular contribution over structural diffusion increased with increasing the cation-anion binding energy in the order: $[Zn(TFSI)]^+ > [Mg(TFSI)]^+ >$ LiTFSI > NaTFSI.[64]

Unlike glymes, a similar contribution of the vehicular and structural was observed for the carbonate-based electrolytes (Figure 9A) in salt-in-solvent and solvated-salts regimes (up to 3 M) and in the solvent-in-salt regime for the AN-based electrolytes.[42,60,61,69,70] Figure 9B demonstrates how the Li^+-solvent and Li^+-anion exchange varies with salt concentration by plotting the average distances a Li^+ travels before exchanging all its solvents, TFSI anion (N of TFSI) and oxygens of TFSI. In the salt-in-solvent regime, the Li-AN move together slightly less than two AN sizes using 5 Å as an estimate of the AN size along the longest dimension. In the solvent-in-salt regime (AN/Li=2), the Li^+ exchanges AN as its moves slightly less than one size of AN, thus suggesting that the solvent exchange becomes dominant. A relatively strong binding of the Li^+ to $TFSI^-$ versus AN results in a slower exchange rate of Li^+ with TFSI anions than with AN solvent, thus, in dilute solutions, the LiTFSI ion pairs move largely via the vehicular mechanism. Multiple exchanges of the Li-O(TFSI) occur before the Li-N(TFSI) dissociates and the anion completely leaves the Li^+. This picture is consistent with suggestion from Yamada et al. that super-concentration might disrupt the vehicular-dominance manner, leading to a repeated ion

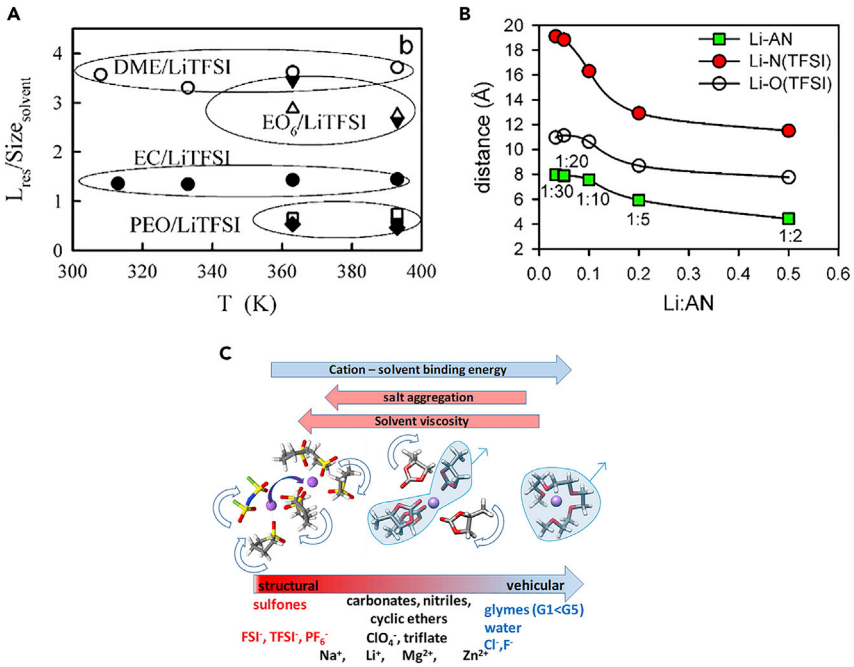

Figure 9. Ion Transport at Super-Concentration

An illustration of the structural (solvent and anion exchange) and vehicular contributions for the cation diffusion.

(A) Distance a Li^+ diffuses without exchanging solvent (during one Li-solvent residence time) for EC, DME, pentaglyme (G5 or $(EO)_6$) and 54 repeat unit PEO/LiTFSI in the salt-in-solvent regime from MD simulations[60] (Copyright Springer 2007 reproduced with permission);

(B) The average distance a Li^+ diffuses without exchanging solvent or TFSI anion nitrogen or oxygen on average using reanalyzed data from Seo et al.[61] as a function of salt concentration;

(C) A summary of parameters influencing the structural and vehicular contribution to the metal cation transport in electrolytes.

association-dissociation process, which is a form of distinct structural diffusion.[21] However, one needs to keep in mind that the structural versus vehicular contributions could be different for the solvent and anions.

Highly viscous and relatively large sulfolane (SL) solvent has two closely spaced solvating oxygens in the $-SO_2$ group (Figure 9C) allowing a Li^+ to exchange them at the same time scale as it moves a size of the SL molecule.[71] A similar Li^+ and solvent diffusion was observed in the salt-in-solvent regime (SL/Li = 8.33), while in the solvent-in-salt regime (SL/Li = 2.56) the Li^+ diffusion was more than 50% higher than SL diffusion from MD simulation predictions,[71] which were confirmed by pfg-NMR measurements.[71,72] A significantly faster Li^+ diffusion than solvent is rare, as typically the Li^+ diffusion is lower than that for the solvent in the salt-in-solvent regime, with few exceptions where it become comparable or only slightly faster.[12,16,63,73]

We summarize main factors influencing the relative contributions of vehicular and structural diffusion to the metal cation transport in Figure 9C. A strong cation-solvent binding, low solvent viscosity (DME or AN) and small solvent size (water) favor the vehicular mechanism, which could switch to structural diffusion as salt concentration increases. One exception is water: even in the water-in-salt regime (21m LiTFSI, H_2O/Li = 2.67), a high fraction of the fast moving solvent-separated

$Li^+(H_2O)_4$ indicated prevalence of the vehicular mechanism as the $Li^+(H_2O)_4$ moved multiple sizes of water molecules before the Li^+ exchanged its solvation shell.

An alternative descriptor related to ionic transport is the Walden analysis, where the correlation between molar conductivity (concentration-normalized conductivity) and viscosity is compared, and a linear relationship in a given concentration range may indicate a well-dissociated electrolyte. According to Yamada et al., the Walden plot of their "hydrate melt" electrolyte, which bears close similarity to WiSE, reveals a pronounced cation-anion decoupling behavior, benefited from the well-dissociated lithium salts in H_2O and strongly suggesting an ionic hopping process.[51,52] From an electrolyte performance perspective, it remains unclear which mode of diffusion is desirable, although Bedrov et al., via molecular dynamics analysis, suggested that a more structural diffusion may allow a higher transference number.[65]

One important ramification of the liquid structure with nano-heterogeneity is the fast Li^+ transport, which is enabled by the high fraction of free Li^+ via a vehicular motion through the water-rich region.[49] Existing as a 3D percolating network in WiSE, and experimentally evidenced by small-angle neutron scattering (Figure 7D),[49] this pathway for fast Li^+ transport originates from the local solvation structure, i.e., the disproportionation in Li^+-solvation sheath structure. Since anions are relatively immobilized by the anion-rich phase, the transport of those Li^+ is preferred, as evidenced by the high Li^+- transference numbers as measured by pulse-field NMR.

Ion Transference Number

Besides ionic conductivity, ion transference number (t_+) is an equally important descriptor for ion transport. While the former defines the overall capability of an electrolyte to provide ionic current, the latter describes the "quality" of such capability, because it quantifies the portion contributed by each ionic species to the overall ionic current, given that for an electrochemical device, only the portion of the current carried by the ions essential to the cell reactions matters. A high t_+ for essential ions implies high rate capability for the resultant electrochemical device, which minimizes the bulk electrolyte resistance under the condition of fast charge or discharge.

In dilute electrolytes based on "good solvents," the ions are effectively screened from their counterions, hence their movements should be considered uncorrelated to interionic effects, and the cation transference number could be approximated using self-diffusion coefficients obtained from MD simulations or pfg-NMR measurements:

$$t_+(\textit{ideal or uncorrelated}) = \frac{D_+}{D_+ + D_-} \qquad \text{(Equation 1)}$$

This approximation, however, breaks down even in dilute regimes whenever there is strong interionic association, examples of which include strongly dissociated salts in poor solvents (such as [alkylpyrrolidinium] [TFSI] in DMC), where ion correlation increases with decreasing salt concentration, in a complete reversal of what expected from a well solvated electrolyte[54] and other strongly aggregating electrolytes even at low salt concentrations such as fluoromethane-THF/LiTFSI[74] or $LiCF_3CO_2$ in AN.[75] Thus, Equation 1 should be applied with caution for those scenarios where interionic attraction cannot be ignored.

A convenient formalism for calculating t_+ was suggested by Wohde et al.,[76] who, based upon Onsager reciprocal relations combined with linear response theory,

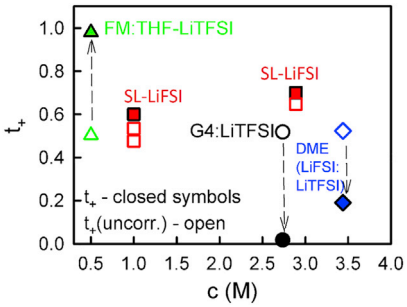

Figure 10. Impact of Super-Concentration on Preferred Ion Transport

Transferance number calculated assuming uncorrelated (ideal) ion motion (t_+(uncorr.)) and correlated using formalizm from Wohde et al.[76] for fluoromethane(FM):THF-LiTFSI,[74] post-processing sulfolane (SL)-LiFSI,[71] 3.46m LiTFSI+ 3.46m LiFSI in DME,[40,67] and G4-LiTFSI (Borodin).

considered two important regimes characterized by their parameter β: (1) a strongly coupled ion and cation motion due to ion pair formation ($\beta \rightarrow 1$) that reduces t_+; and (2) an anticorrelation of the positive and negatively charged current contributions due to Li^+ moving together with a bulky solvation shell in the opposite direction in order to preserve momentum, thus creating an anticorrelation ($\beta \rightarrow -1$).[65]

Dong et al. demonstrated that the t_+ for the salt-solvate electrolyte LiTFSI/G4 (1/1) under anion-blocking conditions can be much lower than t_+(ideal).[55] They reported that the mobility of Li^+ and $TFSI^-$ is similar, leading to t_+(ideal) ≈ 0.5. However, MD simulations and analysis of experiments showed that the anti-correlated motion in combination with anion-blocking condition results t_+ being only (0.02–0.06). Similar result was generated by our simulations (Figure 10). Such behavior is related to the momentum conservation constraint and inability of G4 molecules associated with the Li^+ to support the momentum exchange between ions. This finding indicates that such solvated salt electrolyte cannot support the charge-discharge rates expected from t_+(ideal). In order to overcome this detrimental effect for battery applications, Dong et al.[55] suggested to improve the momentum exchange so that anti-correlated motion of ions could be minimized, which can be realized by (1) diluting electrolyte with additional solvent molecules that are not complexing with Li^+ ions; or (2) decreasing the residence time for solvent molecules near Li^+ so that the ionic transport mode is switched from vehicular to structural. The latter can happen when the short-chain glyme molecules or carbonates are used.[60] In both approaches, solvent molecules facilitate momentum exchange in the system and therefore the momentum conservation in the system can be accomplished without strong dynamic correlations between ions.

A significant increase in t_+ from 0.02 to 0.19 is indeed realized when a longer glyme G4 is replaced with a shorter glyme (G1, DME), and a smaller salt (LiFSI) is introduced as a bi-salt electrolyte (Figure 10). The faster Li^+ exchange as compared to longer glymes,[60] and shorter residence time of LiFSI versus LiTFSI by a factor of two at room temperature partially switched the Li^+-transport mechanism from the vehicular to structural, resulting in much higher t_+ despite higher concentration of salts (3.4 M LiTFSI-LiFSI in DME versus 2.8 M LiTFSI in G4). High contribution of the Li^+-solvent exchange and faster Li^+ than solvent diffusion lead to not only t_+ (ideal) but quite unusually to t_+ being higher than 0.5 for the SL/LiFSI electrolyte. Unlike a strongly decreasing t_+ with increasing salt concentration for the G4-LiTFSI electrolyte, an inverse trend of a slightly increasing t^+ observed for SL/LiFSI during additional analysis of MD simulations.[71] Using small and light water molecule compared to the much larger and heavier glymes present an alternative strategy to improving t_+ compared to t_+ (ideal) in the super-concentrated regime. Preliminary analysis of the extended

MD simulations of 21m LiTFSI in water using APPLE&P force field indicate that the presence of strong but small and light solvent water still manages to ensure a much weaker anticorrelation with the $TFSI^-$ anions, as evidenced by the t_+ of 0.32–0.36 that is much higher than 0.02–0.06 reported for G4-LiTFSI.

Thus, the effect of super-concentration on t_+ is by no means monotonous. Extremely low t_+ occurs with the formation of large Li^+-solvates, as in the case of salt-solvates by ether solvents. Although these solvated species are well separated from anions by the strong solvating molecules, the long residence time of the solvents make the solvated Li^+ rather clumsy in motion. Introducing ligands that could be rapidly exchanged, such as light and strong solvent (water) or strongly dissociating anion (FSI) could lead to t_+ even higher than t_+ (ideal).

As salt concentration decreases in good electrolyte, one expects t_+ to approach t_+ (ideal) due to decreased ion correlation as solution becomes more dilute. However, a recent report that the strong ion correlations lead to t_+ being higher than t_+ (ideal) at low salt concentration fluoromethane(FM):THF-0.5 M LiTFSI electrolyte is quite intriguing.[74] This large and positive deviation from non-ideality is clearly due to ion aggregation, specifically due to formation of the large negatively charged slow-moving clusters containing an excess of $TFSI^-$ and solvent separated Li^+ solvates that diffuse fast in a low viscosity FM solvent. Despite similar average self-diffusion coefficients for Li^+ and $TFSI^-$, the diffusion of the solvent separated Li^+ is 2–2.5 times faster than the average diffusion coefficients of all Li^+ and $TFSI^-$ anions. The much higher fraction of free Li^+ as compared to free $TFSI^-$ indicates a high contribution of Li^+ to the electrolytic conductivity compared to anion contribution that move slower and essentially do not exist as free ions. Experimentally, a slightly smaller value of $t^+ = 0.79$ was measured using the potentiostatic polarization method but it indicates experimentally that t^+ for low salt concentration could be above 0.5, albeit it is unusual.

INTERFACIAL STRUCTURE AND INTERPHASIAL CHEMISTRY

Among the "unusual" properties brought by super-concentration, perhaps the most important is the new interphasial chemistries that differ from the non-concentrated systems. Such new interphases are already recognized as the key to enable electrochemistry at extreme potentials, and examples include the super-concentrated ethers, sulfone, sulfoxide, nitriles, and even water, which form protective interphases on various electrode materials and make them reversibly functional at potentials otherwise impossible. All these new interphases now bear chemical signatures from the anions instead from the solvent molecules, unlike dilute electrolytes whose interphasial chemistry are primarily dominated by the reduction or oxidation of solvent molecules. It was this new chemical reliance of interphase on anion instead of solvent molecules that lifts the many traditional confinements imposed on electrolyte design, the most conspicuous of which is ethylene carbonate (EC), the indispensable solvent in electrolytes for any LIBs manufactured nowadays, primarily because of its key role in forming interphase on graphitic anode.[43,59]

Although a correlation has been established between Li^+-solvation sheath and the interphase assuming a transition state of Li^+-solvent co-intercalation into graphite,[59] predicting interphasial chemistry has been, and still is, challenging. In a more general context, it is reasonable to assume that before the potential of a certain electrode reaches the threshold value of "breaking down" electrolyte components,

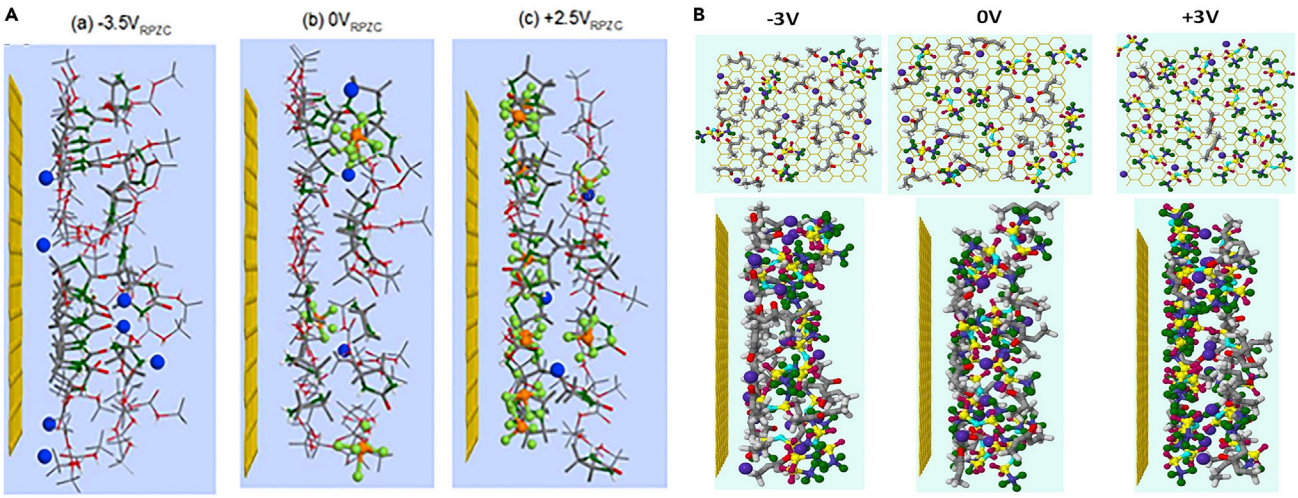

Figure 11. New Interfacial Structures at Super-Concentrations

(A and B) Double layer structure for the salt-in-solvent 1M $LiPF_6$ in EC:DMC(3:7) (A) and solvent-in-salt $DMC_{1.2}TFSI$ electrolytes (B) from MD simulations.[80,81] Copyright American Chemical Society 2012 and 2017. Reproduced with permission.

where *interphasial* chemistry starts, there should be already an *interfacial* structure existing at the so-called inner-Helmholtz layer. This self-assembly of electrolyte components, enriched in certain components while deprived of the others, should be the immediate parental entity that dictates the eventual interphase. Hence, understanding its chemical composition and structure might provide the key knowledge to predict interphase chemistries.[31,74,77–80]

Consider a graphitic anode in a typical carbonate electrolyte (~1.0 M $LiPF_6$) is being charged for the first time. At the moment, although its surface is free of any interphase, an interfacial assembly has already built up due to contact with electrolyte. As the graphite is negatively polarized, this interfacial assembly at inner-Helmholtz layer should gradually become enriched with Li^+,[81,82] along the solvent molecules in the Li^+-solvation sheath. These solvent molecules are made susceptible to reduction more than other species, because of their close proximity to the anode surface and the activation of the bonds within them by Li^+. Meanwhile the anions would be pushed away to the outer-Helmholtz layer by the anode surface due to increasing negative charges, forming an electric double layer structure with distinct cation-rich and anion-rich regions (Figure 11A).

Such an inner-Helmholtz structure will be disturbed by the change of the salt concentration in the electrolyte. The super-concentration would compress the thickness of the inner-Helmholtz layer and force the anion to approach the anode despite the coulombic expulsion (Figure 11B). The consequence of such an interface with higher anion population and Li-Anion aggregation certainly increases the chances of anion-reduction due to excess electron stabilization when the anion is coordinated with one or multiple Li^+ or other cations,[24,26,27,83] which often increases the reduction potential of anions. Thus, super-concentration provides a viable option to manipulate interphasial chemistry by switching its potential source from solvent molecules to anions.[21,22,24,26,27,41,71,84–87]

Similar process happens on the cathode surface. MD simulations revealed that anion concentration increases in the inner-Helmholtz layer as an electrode becomes positively polarized.[81] When electrolytes are based on mixed solvents, such as the

typical formulations used in commercial LIBs, a preferential partitioning of EC versus DMC or other linear carbonates at both negative and positive electrodes increases its opportunity of participating SEI and CEI formation.[81] Both solvent and anions are found in the inner-Helmholtz layer next to cathode surface when the salt concentration is ~1.0 M,[81] while super-concentration or ionic liquids completely populate the inner-Helmholtz layer and expel all solvent molecules away from the cathode surface, screening them from possible oxidation.[52,78–80] The anion structure also plays a role in deciding if preferential adsorption could occur. For example, MD simulations[79] found that TFSI seems to be favored over trifluoromethane sulfonate (OTf) during positive electrode polarization from potential of zero charge, which has been confirmed by the surface-enhanced IR spectroscopy.[80]

Compared with the cathode, which attracts anions due to its positive-charged surface, the intrinsic repulsion of anions by the negatively charged anode creates the so-called "cathodic challenge," which makes the anion-derived SEI more challenging than CEI.[31] When an extremely negative potential is applied, even the super-concentration cannot overcome the strong repulsion in order to populate the anode surface with sufficient anions required for SEI formation. Cationic species such as $Li^+(H_2O)_n$ in the WiSE would eventually appear at the anode surface, resulting in water reduction and preventing formation of a stable SEI.[79] This difference between the anode and cathode surfaces in their preferred inner-Helmholtz structure constitutes the fundamental reason for the strong "positive bias" observed for the expanded electrochemical stability window for WiSE and its derivatives -(hydrate melt, water-in-bisalt, etc.), leaving anode as the most challenging component to stabilize in aqueous electrolytes.[33]

In their initial publication, Suo et al. described the chemical composition of the aqueous SEI formed in WiSE as neat LiF, which was confirmed by various spectra including chemical analysis via EDX under TEM, XPS[24] as well as SIMS.[77] This conclusion seemed to be reasonable, because LiF is the least soluble lithium salt in water,[88] which makes it an excellent candidate as component of aqueous SEI. Quantum chemistry calculations predicted LiF formation to occur as a result of Li_2TFSI reduction above 2.4 V versus Li/Li^+, while the Li_2TFSI reduction coupled with the S–N bond breaking being kinetically more favorable below 2.1 V versus Li/Li^+.[24,80] The anion defluorination coupled with reduction was also observed in the sodium version of WiSE, where the SEI identified on the surface of the cycled anode seems to be even more pure NaF with clear lattice structure matching the crystal database. In a more detailed mechanism study, Suo et al. further established the correlation between the hydrogen evolution and the LiF formation during the first charging cycle,[77,89] while sequential bombardment of the formed SEI by Ga^{3+} revealed the presence of minor Li_2O and Li_2CO_3 in addition to the major component LiF. They attribute the formation of Li_2O and Li_2CO_3 to the reduction of water and the trace amount of CO_2 dissolved in WiSE.

More recent studies challenged the SEI formation mechanism in WiSE that has been centered on direct electrochemical reduction of TFSI. Dubouis et al. proposed that the free, unbound water molecules plays the key role, which electrochemically reduce to hydroxide accompanied by hydrogen evolution during the first charging.[89] TFSI then undergoes nucleophilic attack by hydroxide, chemically decomposes, and lead to LiF or NaF deposited on anode surface as eventual interphasial components. Lee et al. even claimed that an aqueous SEI does not necessarily require the anion to provide chemistry source. By using a super-concentrated

(17 m) electrolyte based on $LiClO_4$, they showed that interphases were formed with Na_2CO_3 and NaOH as the main components, without apparent participation from the anion.[90] Thus, Lee et al. attributed this new interphasial chemistry to the oxygen and CO_2 dissolved in the WiSE, which had been recognized earlier by Suo et al. but were not thought to be the chemical basis for an interphase.[24] Zheng et al. further argued that the main contribution to the expansion of electrochemical stability window could be the result of neat kinetic barrier for a water molecule to free itself from a polymer-like local structure $[Li^+ (H_2O)_2]_n$ in WiSE.[91] Given the fundamental importance of this topic, more debate and intensive research are likely.

Finally, in order to overcome the cathodic challenge, so that an electrochemical stability of >4 V could be established for aqueous electrolytes, Yang et al.[31] leveraged the two characteristics of fluorinated ethereal compounds: (1) they are hydrophobic by nature, so they can effectively shield the anode surface by pushing water molecules away from the inner-Helmholtz layer before interphase formation; and (2) they are active toward electrochemical reduction like their carbonate counterparts FEC or FEMC, which generates LiF as well as numerous fluorocarbon species that a new interphase could use as chemical building blocks. Under the protection of this new interphase, a graphitic anode can be lithiated to its 1st stage, delivering a specific capacity of ~300 mAh/g and enabling a 4 V class aqueous Li-ion battery for the first time. This technique provides the foundation for high voltage aqueous battery chemistries that could eventually compete with state-of-art Li-ion batteries in terms of energy densities.[32]

SUPER-CONCENTRATION AND BATTERY PERFORMANCES

With only a few exceptions, where super-concentrated electrolytes were used as synthesis media, or supporting electrolytes for electrochemical actuators, sensors or electrodeposition,[92–94] majority of the efforts to explore super-concentration were driven by their potential applications in energy storage systems, batteries in particular. Some of the benefits brought by super-concentration has been described in previous sections when discussing their related properties (Figure 4C). This section intends to be a more systematic, but by no means thorough, summary by examining the three representative battery chemistries where super-concentrated electrolytes have been applied.

Li-Ion Chemistries

The definition of Li-ion chemistries is not always constant. As a commercialized product, its narrow definition refers to dual-intercalation electrochemical cells constructed upon graphitic carbon anode and diversified transition metal cathode, while in research community a broader definition apples to any electrochemical cells that involve Li^+ but not Li-metal. Given the mature nature of commercial Li-ion batteries, whose components have experienced lengthy refinement and synchronization,[95] there is little space for super-concentrated electrolytes to outperform the current carbonate-based electrolyte systems. Thus, the early work on ether-, sulfoxide or acetonitrile-based electrolytes aimed to demonstrate certain unusual properties brought by the super-concentration as novelties rather than proposing these as replacements for the carbonate-based electrolytes.[12,20,22,96] After all, the ability of these exotic solvents in stabilizing graphitic anode was not necessarily superior to what state-of-the-art EC-based electrolytes can do.

The real value of these super-concentrated electrolytes for Li-ion batteries hence lies in whether they can deliver what the carbonates cannot in one or more key

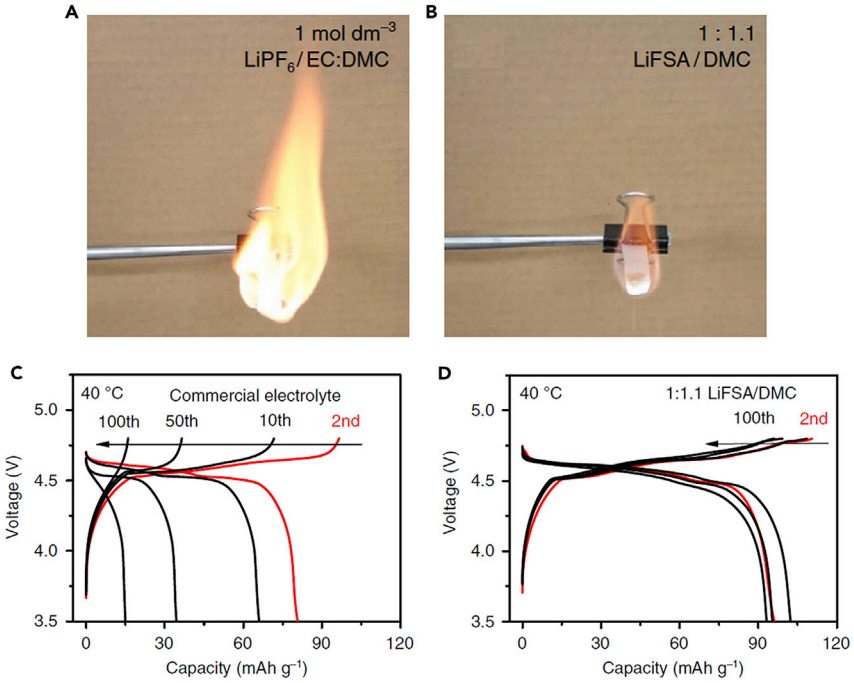

Figure 12. Super-Concentrated Electrolyte of Non-flammability and High Voltage Stability
(A and B) Flammability test of baseline electrolyte 1.0 M $LiPF_6$ in EC/DMC and super-concentrated electrolyte consisting of LiFSI in DMC; the corresponding electrochemical performances of baseline electrolyte and LiFSI/DMC (C and D) in a full LIB consisting of natural graphite anode and $LiNi_{0.5}Mn_{1.5}O_4$ cathode. Reproduced with permission from Wang et al.[22] Copyright Springer Nature 2016.

properties while maintaining comparable performance with carbonates in the rest. This strategy became clear in later efforts by Yamada et al., who proposed a super-concentrated DMC solution of LiFSI, which not only supports a high voltage Li-ion cell constructed on $LiNi_{0.5}Mn_{1.5}O_4$ cathode and natural graphite, but also remain fire-resistant (Figure 12),[22] and later on by Alvarado et al., who proposed a carbonate-free system based on sulfolane to support the same Li-ion chemistry.[71] Unlike carbonate solvents, which releases CO_2 upon oxidation, sulfolane prefers to polymerize following its oxidation coupled with the H-transfer to cathode surface, forming a nanometric interphase. Li-ion pouch cells using such electrolyte have been verified to experience little or no volume expansion during long-term cycling at elevated temperatures.

Super-concentration also makes the Li-ion chemistry aqueous. The interphase formed on anode surface by the extremely high (21 m) anion concentration significantly expanded the electrochemical stability window of aqueous electrolytes to the realm of 3 V, enabling a series of 3-V class chemistries[24–26,97,98] With the application of a hydrophobic interlayer, the electrochemical stability window of aqueous electrolytes can even be further expanded to >4.0 V, enabling cells using graphitic anode and delivering comparable energy density as the state-of-the-art Li-ion batteries (Figure 13).[31] The aqueous nature of such cells brings unprecedented flexibility, tolerance against mechanical abuses, and freedom in cell form-factor (Figure 14), making the open cell configuration possible.

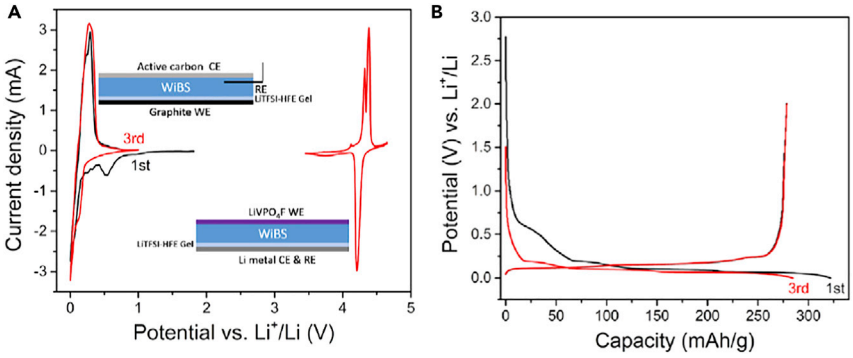

Figure 13. High Voltage Aqueous Electrolytes: A 4-V Aqueous LIB Enabled by Protected Graphite Anode in WiSE

(A) Cyclic voltammograms of a graphite anode pre-coated with LiTFSI-HFE gel, which shows full lithiation of graphite at <0.5 V versus Li. Also displayed in the figure on anodic side is the CV of a $LiVPO_4F$ cathode. All CVs were obtained at the scanning rate of 0.5 mV/s. Insets are schematic illustrations for the cell configurations used in anode and cathode.

(B) Charge and discharge voltage profiles of graphite electrode pre-coated with LiTFSI-HFE gel under galvanostatic condition. Reproduced with permission from Yang et al.[31] Copyright Cell Press 2017.

Beyond Li-Ion Chemistries

Sodium-Ion Batteries

The relatively low solubility of sodium salts as compared with their lithium cousins make it more difficult to formulate sodium version of the super-concentrated electrolytes in either carbonate or ether solvents, therefore judicious choice of solvents and salts constitutes the key to success. For example, Takada et al. reported the combination between NaFSI and a nitrile solvent, succinonitrile (SN), where the salt concentration reached ~50% mol.[99] This high concentration enabled the formation of an anion-originated interphase on hard-carbon anode, which brings excellent cycling stability to the Na/hard-carbon half cell.

The excellent solvation power of water relieves the solubility limitation on most sodium salts, giving much more formulation opportunities to sodium version of the super-concentrated electrolytes. Even so, the maximum concentration of NaTFSI (~9 m) achieved in water is still far lower than WiSE based on LiTFSI (21 m).[27] Nevertheless, this concentration is sufficient for the formation of a NaF-dominated interphase on $NaTi_2(PO_4)_3$ anode, offering a 2.5 V electrochemical stability window. In sharp comparison, 9 m LiTFSI was insufficient to form an effective interphase.[24] Molecular dynamics attributed this lower concentration threshold for interphase formation to the stronger tendency toward ion aggregation in sodium salts, consequently a dense interphase could be formed at lower anion population in the bulk electrolyte. A full Na-ion battery constructed on $Na_{0.66}[Mn_{0.66}Ti_{0.34}]O_2$ as cathode and $NaTi_2(PO_4)_3$ anode was demonstrated with excellent cycling stability. In an alternative approach, $NaClO_4$ was able to be dissolved in water at 17 m, yielding an electrochemical stability window of 2.7 V, although now the interphase no longer came from the anion reduction.[90] Instead, an interphase consisting of Na_2CO_3 and NaOH supports the full-cell constructed upon $Na_4Fe_3(PO_4)_2(P_2O_7)$ cathode and $NaTi_2(PO_4)_3$ anode with excellent cycle stability and a coulombic efficiency of ~99%, which outperforms the sodium version of WiSE based on the more expensive salt NaOTf.

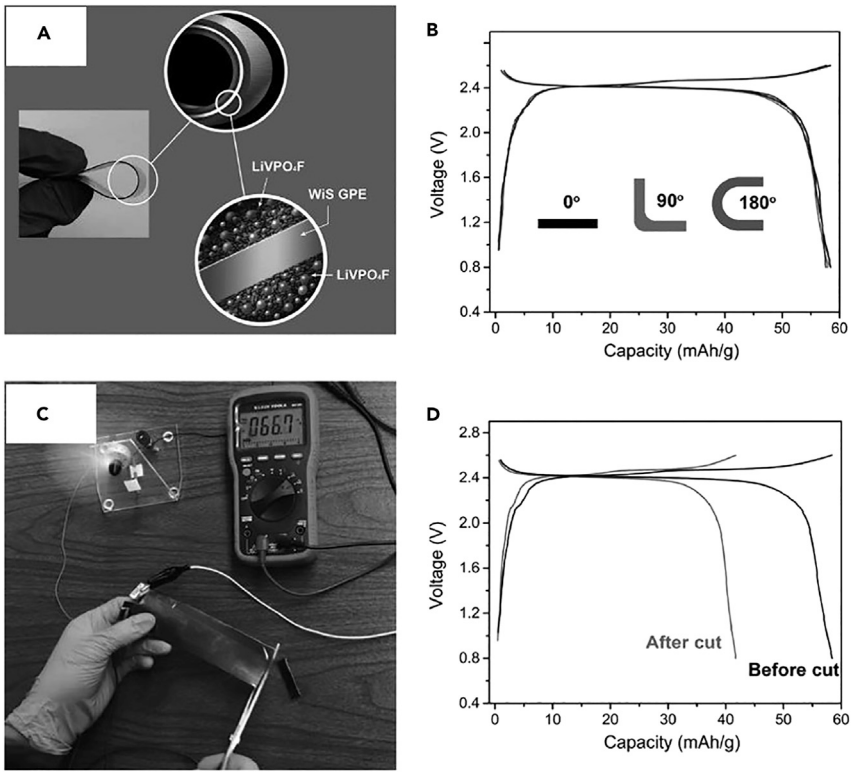

Figure 14. Aqueous Batteries of High Flexibility and Mechanical Tolerance

(A) Full aqueous LIB constructed with a symmetric electrode Li_2VPO_4F shaped in belt and its mechanical flexibility;

(B) The voltage profiles of the flexible battery at 2 C under different under various deformation angles; (C) the robustness demonstration of aqueous flexible LiVPO4F cell that powers a fan of 160 mW while being cut in the open air. The reading of amperemeter is 66.7 mA. The cell survived cutting while continuing the operation in the open environment.

(D) The voltage profiles of the flexible battery at 2 C before and after being cut. Reproduced with permission from Yang et al.[97] Copyright Wiley 2017.

Li-Sulfur Batteries

Li-sulfur chemistry promises tantalizing energy densities but encounters key challenges: (1) the dissolution of the intermediate polysulfide species and the consequent parasitic shuttling; (2) the electronically insulating materials at both fully charged (S_8) and fully discharged states (Li_2S); and (3) the Li-metal anode instability. While the latter two cannot be resolved via electrolyte engineering, the first definitely requests new electrolyte formulations.

Most carbonate solvents are considered reactive with most of these polysulfide species, which were irreversibly turned into thiocarbonates, while ethers of various lengths have been used as mainstream solvents. However, although ethers are non-reactive with polysulfides, they dissolve polysulfides at high concentration and hence encourage parasitic shuttling. In one of the early efforts at super-concentrated electrolytes, Suo et al. dissolved 7 m LiTFSI in an ethereal mixture consisting of DME and DOL, and found that the solubility of polysulfides was significantly suppressed.[20] The near elimination of polysulfide shuttling is evidenced by the coulombic efficiency nearing 100% and long cycling stability. Polysulfide dissolution is further suppressed by CEI formation on the carbon-sulfur cathode as a result of higher reduction potential of LiFSI salt observed in the concentrated electrolyte

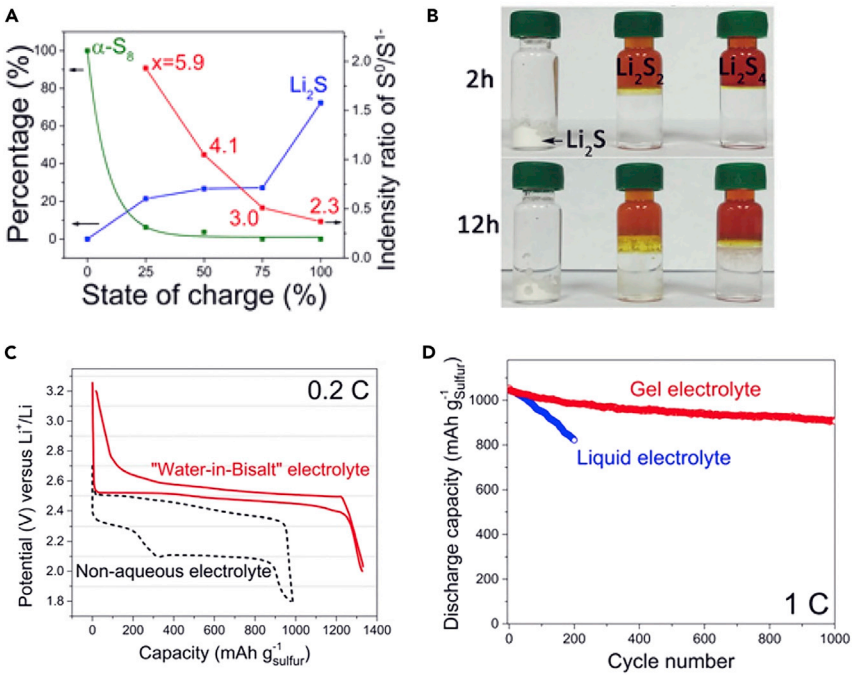

Figure 15. Super-Concentrated Aqueous Electrolyte for a Unique Sulfur | Li-Ion Chemistry

(A) The suppression of polysulfides in WiSE as evidenced by the estimated content ratios of element S_8 (green), Li_2S (blue), and LiPS at specific states-of-charge.

(B) Visual observation of the insolubilities for Li_2S and short-chain polysulfides (Li_2S_2 and Li_2S_4) in WiSE; A Li_2S white powder remains insoluble in clear aqueous electrolyte for 12 h. Jacinth solution on the top of bottle is Li_2S_2 or Li_2S_4 dissolved in water phase, which is separated from the clear aqueous electrolyte (salt phase) on the bottom. The electrochemical performance of sulfur | Li-ion full cells constructed with sulfur-carbon black anode and $LiMn_2O_4$ cathode.

(C) Comparison of the electrochemical behaviors of sulfur composite electrode in non-aqueous and super-concentrated aqueous electrolytes at 0.2 C.

(D) Cycling performance of aqueous sulfur | Li-ion full cells in liquid WiSE and its gel at 1 C.

Reproduced with permission from Yang et al.[29] Copyright National Academy of Sciences 2017.

regime.[83] Watanabe showed that the highly concentrated SL-LiTFSI supports higher rates of the Li-S cell cycling compared to concentrated ethers due to higher t_+ of the SL-based electrolytes discussed above while suppressing polysulfide dissolution, especially when a localized concentrated electrolyte concept is applied by mixing SL-LiTFSI with the highly fluorinated ether.[100] This approach can also be viewed as an extension of the sparingly solvated approach to limit polysulfide dissolution.[101]

An interesting twist of Li-sulfur chemistry was reported by Yang et al., who realized that, although the cathodic stability limit of WiSE cannot directly accommodate Li-metal, it can do so with sulfur. Therefore, they used sulfur (S_8) as a high capacity (1327 mAh/g) anode instead of a low voltage cathode. By coupling this anode with a high voltage cathode such as $LiCoO_2$ or $LiMn_2O_4$, a 2.5 V full "Li-ion" cell is constructed (Figure 15).[29] Such novel electrochemical coupling not only circumvents the Li-metal instability issue that still plagues conventional Li-sulfur systems, but also resolves the dissolution and shuttling issues of polysulfides. The high reversibility of such sulfur anode in super-concentrated aqueous electrolyte enables a unique Li-ion/sulfur chemistry of high energy density (200 Wh/Kg) of excellent cycling stability, which was evidenced by ~100% coulombic efficiency during the 1,000 cycles.

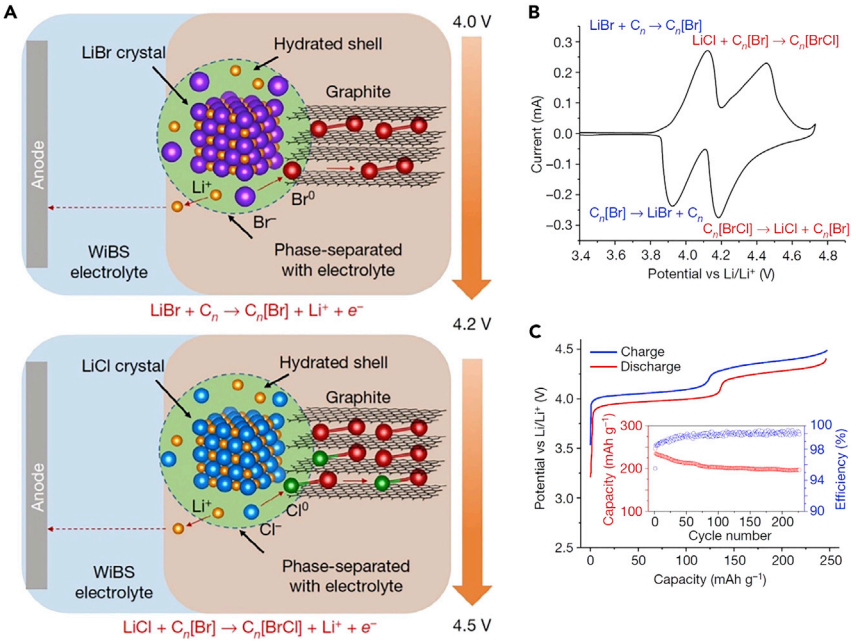

Figure 16. A New Cathode Chemistry Based on Anion Intercalation-Conversion in Graphite and Enabled by WiSE

(A) The proposed intercalation/converstion mechanism that occurs at 4.0 and 4.2 V versus Li, where the stage I intercalation compound of $(Br\text{-}Cl)_{0.5}C_{3.5}$ was formed. The hydration interlayer formed by the halides and WiSE plays the key role in ensuring the reaction proceeds in a reversible manner.

(B) The corresponding cyclic voltammetry performed on a graphite-halide composite electrode in WiSE at 0.05 mV/s.

(C) The galvanostatic cycling of the graphite-halide composite electrode in WiSE at a current density of 80 mA/g. Reproduced with permission from Yang et al.[32] Copyright Springer Nature 2019.

Another innovative aqueous battery chemistry was also reported by Yang et al., who designed an intercalation-conversion mechanism for simple halide anions (bromide and chloride) with graphite,[33] whose capacity (243 mAh/g, corresponding to $(Br_{0.5}\text{-}Cl_{0.5})C_{3.5}$) could outperform most of the transition metal oxides. Here, super-concentrated aqueous electrolyte plays a few key roles: (1) it provides an anodic stability window that can accommodate the high potential (up to 4.5 V) of this intercalation-conversion chemistry; (2) it creates a hydration layer on the surface of the halides confined at the graphite cathode; and (3) most importantly, the halides and halogens do not dissolve in WiSE due to the high salt concentration of bisalts (LiTFSI and LiOTf). When coupled with a protected graphitic anode, this new aqueous battery chemistry delivers undoubtedly the highest energy density known so far for any aqueous batteries (Figure 16).

Li-Air/Oxygen Batteries

Li-air chemistry promises higher energy density than Li-sulfur, but also faces more severe challenges.[102] Beside the Li-metal anode instability issue, researchers have identified electrolyte as a key component that determines if reversible reduction products (peroxides or super-oxides) of oxygen are formed. Because of the high reactivity of oxygen or its radicals toward organic compounds, few non-aqueous solvents are known to meet the stringent requirements.

Considering that water molecules would be stable against peroxides or super-oxides, and their excellent solvating power should lead to effective solvation of the

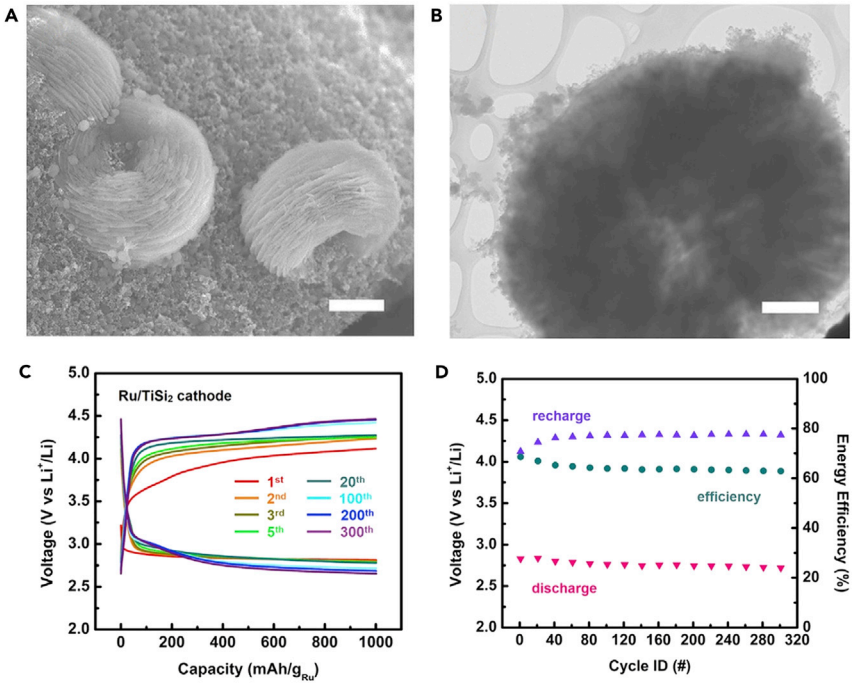

Figure 17. Super-Concentrated Electrolytes for Li-Oxygen Battery

The discharged products on cathode surface was revealed by (A) SEM (scale bar, 2 μm) and (B) TEM (scale bar, 500 nm) to be exclusively Li_2O_2 as evidenced by its typical toroid crystals; the voltage profiles (C) and cycling stability (D) of a Li-O_2 battery constructed with $LiFePO_4$ as a pseudo anode, a non-carbon Ru-based cathode and WiSE. Reproduced with permission from Dong et al.[103] Copyright Cell Press 2018.

intermediate species (super-oxides) that are extremely reactive toward organic compounds, Dong et al. applied WiSE to Li-O_2 cell, in expectation that water molecules should be kept busy with the solvation of both cation (Li^+) and anion (TFSI), so that their electrochemical stability at super-concentration (21 m) should be sufficient to accommodate the redox potential of oxygen. They found that Li_2O_2 was almost the exclusive product formed reversibly on cathode surface during the cell cycling, as evidenced by the toroidal crystals revealed under both scanning and transmission electron microscopes (Figures 17A and 17B),[103] while little LiOH can be detected thanks to the reduced water activity. The elimination of these parasitic by-products brought superior cell reversibility and kinetics (Figures 17C and 17D), although it also brought the inconvenience that now Li-metal anode cannot be directly used in such aqueous electrolytes without additional protection.

Multi-valent Cation Batteries

Cations with multi-valence (>1) have always been tantalizing chemistries to explore, because the coulombic capacity is proportional to the number of electrons transferred per ion during the cell reaction. However, with multi-valence also comes tremendous challenge, because with the formal charge doubled or tripled on an ion of approximately the same or even smaller size (90 pm for Li^+, 86 pm for Mg^{2+}, 114 pm for Ca^{2+}, 88 pm for Zn^{2+}, and 67.5 pm for Al^{3+}), the coulombic resistances the ion encounters, either in bulk electrolyte, in cathode or anode lattices, or in the interphases would be almost insurmountable. This has constituted the largest barrier for the multi-valence battery chemistries that universally exist in

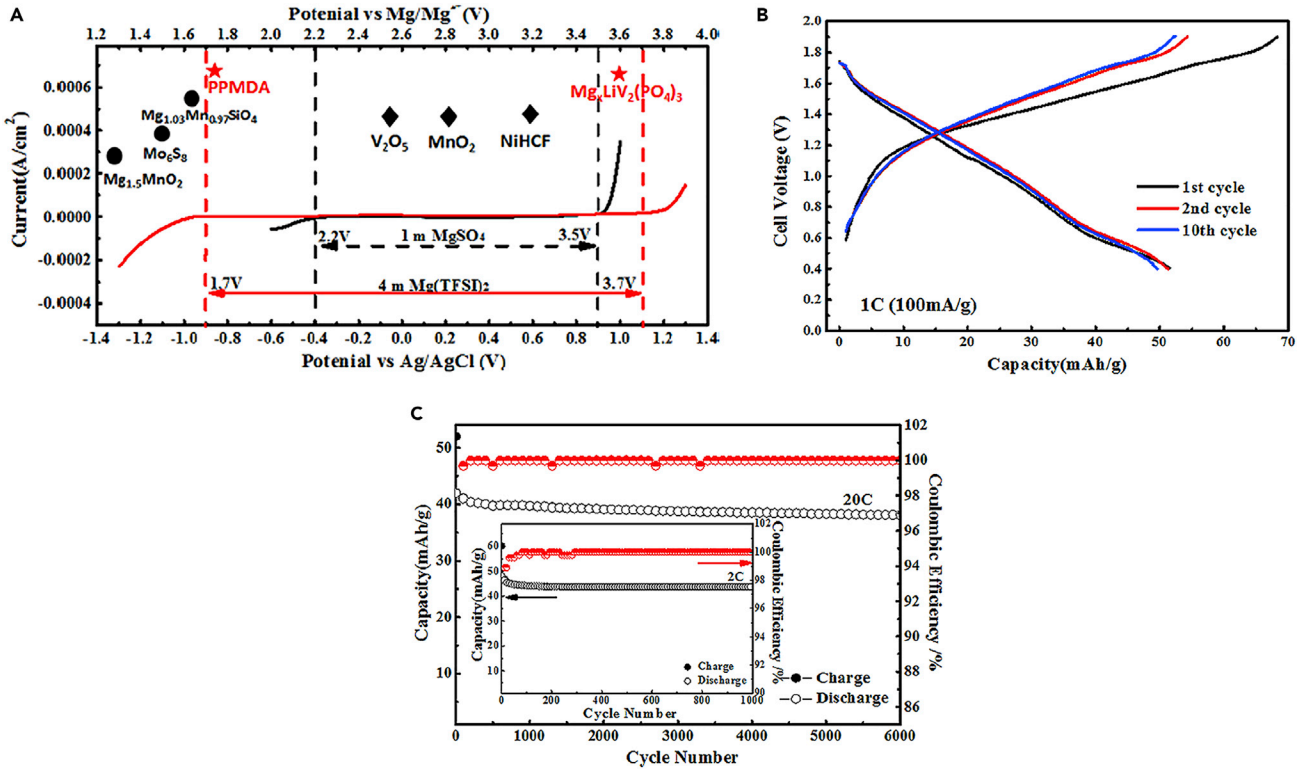

Figure 18. The Super-Concentrated Mg Electrolyte

(A–C) (A) the expanded electrochemical stability window of 4 m $Mg(TFSI)_2$ as measued on stainless steel electrodesat 10 mV/s; (B) the typical voltage profile at 1 C and (C) cycling stability at 20 C of an aqueous Mg battery constructed with polypyrometallic dianhydride anode and vannadium phosphate cathode. Reproduced with permission from Wang et al.[105] Copyright American Chemical Society 2017.

the developments of electrode materials or electrolytes, and in particular interphases. A general consensus existing in the field is that, once a passivation interphase forms, the passage of multi-valence cations would be entirely blocked. This belief has been challenged by a few recent advances,[104] but even in those cases, the transport of multi-valence cations through an interphase would still be regarded as the most resistive process in the battery. Because of these restrictions brought by multi-valence, any attempt to formulate electrolytes for these multi-valence cations has to consider the thermodynamic stability of the components (solvents, salt anion) against decomposition. This restriction becomes especially harsh for Mg^{2+} with a redox potential only ca. 0.65 V above Li, where most non-aqueous solvents would be reduced and form an interphase. Thus, exotic electrolyte systems based on organo-magnesium salts dissolved in ethereal solvents were often used to circumvent the interphase challenges, with compromises in oxidation stability. As result, super-concentrated electrolytes were rarely applied on these multi-valence chemistries, with only a few exceptions.

Wang et al. transplanted the super-concentration concept from WiSE, and reported that an expanded electrochemical stability window of >2.0 V was achieved by dissolving 4.0 m Mg salt in water. Although the cathodic stability limit of this electrolyte is still not low enough to allow for Mg deposition and stripping, its stability window width can comfortably accommodate a full Mg-ion battery using a poly(pyrometallic dihydride) anode and a lithium vanadium phosphate cathode with astonishing cycling stability up to 6,000 cycles (Figure 18).[105] Here the aqueous

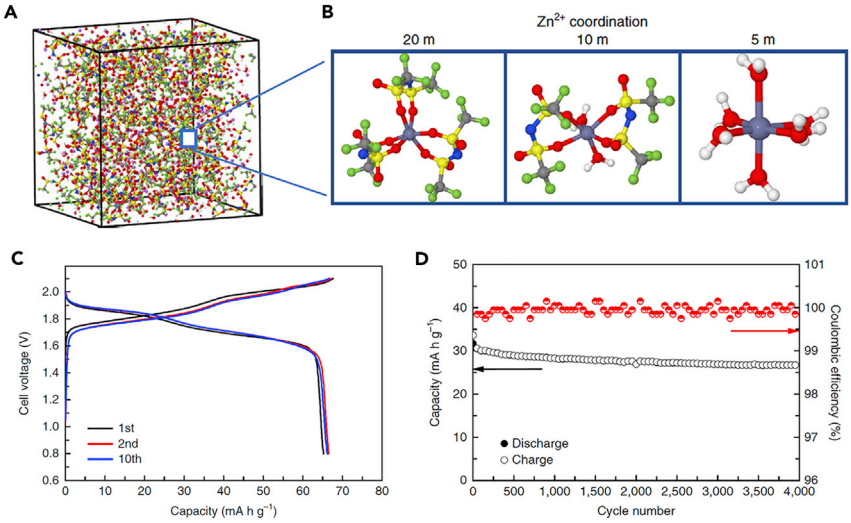

Figure 19. Super-Concentrated Zn Electrolyte (1 m $Zn(TFSI)_2$ in 20 m LiTFSI)
Snapshot from MD simulations (A) and representative average Zn^{2+}-solvation sheath structures in 3 concentrations (B); the voltage profile of a $LiMn_2O_4$/Zn full cell (C) and its cycling stability (D) at constant current (0.2 C). Reproduced with permission from Wang et al.[28] Copyright Springer Nature 2018.

nature of the electrolyte assisted the sluggish migration of Mg^{2+} in its intercalation process in both anode and cathode host lattices, as evidence by the high power density (6,400 W/kg) delivered by the full Mg-ion cell.

The higher redox potential of Zn (2.27 V versus Li) makes it possible to deposit and strip Zn in the aqueous electrolytes. However, the reversibility of Zn, like Li, also suffers from the dendrite formation and sustained reaction between Zn and water. Leveraging the "inert" nature of water in WiSE (21 m LiTFSI in water), Wang et al. dissolved 1 m $Zn(TFSI)_2$ in it, and found that Zn becomes highly reversible, with ~100% coulombic efficiency.[28] They attributed this drastic change in Zn deposition behavior to the new solvation sheath of Zn^{2+} in WiSE (Figure 19), which would consist entirely of TFSI anion because of the fierce competition from the overwhelming Li^+ that would recruit majority of the water molecules. This dendrite-free Zn plating and stripping allows for high reversibility of cells based on a Zn-metal anode and either $LiMn_2O_4$ or O_2 cathodes for up to thousands of cycles.

Li-Metal Reversibility

If Li-metal is the "Holy Grail" for batteries, its reactivity with electrolytes certainly constitutes the Sin that must be overcome before any practical and safe application can be considered. Since its revival in 2010s,[106] diversified electrolyte systems have been explored to mitigate the growth of SEI and the subsequent Li-dendrite and "dead Li".[107,108] Suo et al. perhaps were the first to notice that super-concentration of lithium salt in the electrolyte could regulate the growth of Li crystal in a more orderly manner, although in that case the effect of sulfur or polysulfide cannot be completely ruled out.[20] This was further supported by numerous work that show high salt concentration often leads to higher F-content in the interphase, which might be responsible for this more regulated growth of Li.[40,83,84,109–111] These efforts steadily push up the coulombic efficiencies of Li deposition and stripping, with the newest number being 99.5%,[111] which was realized in a localized

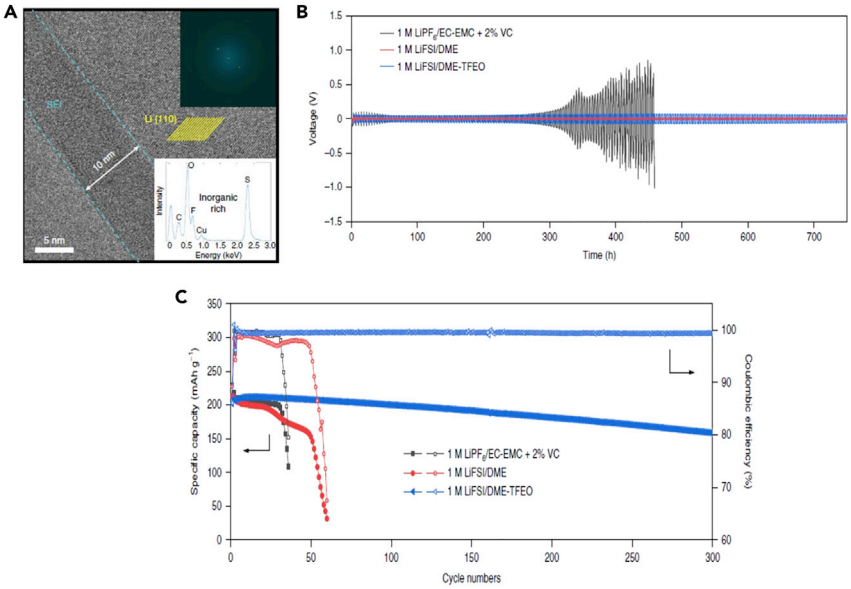

Figure 20. Super-Concentration Enhances Li-Metal Reversibility

Cryo-EM image of Li deposited on Cu grid (A), where the yellow lines delineate the lattice space of the crystalline Li; the electrochemical performances of a Li/Li symmetric cell (B) and a Li/NMC811 full cell (C) using baseline electrolyte and electrolytes containing various additives as labelled. Reproduced with permission from Cao et al.[111] Copyright Springer Nature 2019.

super-concentrated electrolyte with the non-solvent tris(2,2,2-trifluoroethyl) orthoformate (TFEO). This non-solvent ensures the formation of highly homogenous, highly fluorinated, and monolithic SEI and CEI, differing from the known mosaic or layered interphases observed thus far (Figure 20A). Such unique interphases supported the reversible operation of the aggressive Li-metal battery chemistry that uses a high Ni cathode (Figures 20B and 20C), although further improvements are still needed to reach a comparable reversibility with LIBs.

A NEW HORIZON

The success of Li-ion batteries was mainly built on the intercalation chemistries of Li^+ in different hosts at extreme potentials and the interphases that protects the reversibility of such chemistries. In particular, the composite interphase of organic-inorganic nature on the graphitic anode originated from the electrolyte solvents is characterized by a low interface energy, strong bonding, and a durable mechanical property that effectively accommodates the small volume change (<12%) of graphite, ensuring an incredibly high coulombic efficiency of >99.99% during charge and discharge cycles. Such interphases, unfortunately, do not yet exist for the next generation battery chemistries using much more aggressive materials of extremely high volume changes and extremely high reactivity, such as high Ni-content transition metal oxides, conversion-reaction cathodes such as sulfur, or Li-metal anodes. Among all possible interphase components, LiF is known for the highest interface energy with Li,[112] and can be formed from fluorinated salts, especially when the presence of anion becomes sufficiently high, such as in super-concentrated and localized super-concentrated electrolytes.

Thus, super-concentrated electrolytes bring a unique opportunity to resolve the many new challenges presented by these next generation battery chemistries. Super-concentration does not simply represent dissolving more salt in electrolytes. It

opens up a brand-new horizon, not only for electrolyte materials in batteries but in broader context for solution chemistries, electrochemistries, and processes. By drastically changing the primary solvation environments of ions, super-concentration induces the emergence of a sequence of unusual properties and behaviors, such as long-range liquid structures, preferential ion transport, interfacial structures as well as interphasial chemistries.

One significant barrier standing in front the super-concentration is the high salt concentration itself, which not only induces compromises in conductivity and viscosity, it also drives up the cost of the electrolyte. How to maintain these desired merits of super-concentrated electrolytes while resolving these barriers becomes the focus of future efforts. Using anti-solvents to localize the super-concentration emerges as an innovative pathway, which allows for decoupling bulk, transport, and interfacial properties of an electrolyte from the overall salt concentration, so that each property of electrolytes can be individually adjusted,[113] which is impossible in traditional salt-in-solvent electrolytes.

As the interest in this new approach intensifies, more systems are developed, and in-depth understanding is achieved aided by advanced characterization and computational tools, we expect that more unusual properties beyond the current scope of electrochemistry and energy storage research will be discovered.

ACKNOWLEDGMENTS

This work was supported as part of the Joint Center for Energy Storage Research, an Energy Innovation Hub funded by the U.S. Department of Energy, Office of Science, Basic Energy Sciences. C.W. and K.X. also acknowledge the support from the Office of Vehicle Technologies of the US Department of Energy (DOE) through the Advanced Battery Materials Research (BMR) program (Battery500 Consortium) under contract no. DEEE0008202. The authors thank Dr. Marshall A. Schroeder (ARL) for discussions and Dr. Dongliang Chao (University of Adelaide) for graphics help.

REFERENCES

1. Bard, A.J., and Faulkner, L.R. (2000). Electrochemical Methods: Fundamentals and Applications, Second Edition (John Willey & Sons).
2. Brown, A.P., and Anson, F.C. (1977). Cyclic and differential pulse voltammetric behavior of reactants confined to the electrode surface. Anal. Chem. *49*, 1589–1595.
3. Bockris, J.O.M., and Reddy, A.K.N. (1998). Modern Electrochemistry (Kluwer Academic Publishers).
4. Vayenas, C.G., and White, R.E. (1954). Modern Aspects of Electrochemistry (Butterworth).
5. Vincent, C.A. (2000). Lithium batteries: a 50-year perspective, 1959–2009. Solid State Ionics *134*, 159–167.
6. Ratner, M.A., and Shriver, D.F. (1988). Ion transport in solvent-free polymers. Chem. Rev. *88*, 109–124.
7. McKinnon, W.R., and Dahn, J.R. (1985). How to reduce the cointercalation of propylene carbonate in Li_xZrS_2 and other layered compounds. J. Electrochem. Soc. *132*, 364–366.
8. Angell, C.A., Liu, C., and Sanchez, E. (1993). Rubbery solid electrolytes with dominant cationic transport and high ambient conductivity. Nature *362*, 137–139.
9. Chen, L., Li, Y., Li, S.-P., Fan, L.-Z., Nan, C.-W., and Goodenough, J.B. (2018). PEO/garnet composite electrolytes for solid-state lithium batteries: from "ceramic-in-polymer" to "polymer-in-ceramic". Nano Energy *46*, 176–184.
10. Gupta, A., and Sakamoto, J. (2019). Controlling ionic transport through the PEO-LiTFSI/LLZTO interface. Electrochem. Soc. Interface *28*, 63–69.
11. Jeong, S.K., Inaba, M., Iriyama, Y., Abe, T., and Ogumi, Z. (2003). Electrochemical intercalation of lithium ion within graphite from propylene carbonate solutions. Electrochem. Solid-State Lett. *6*, A13–A15.
12. Ueno, K., Yoshida, K., Tsuchiya, M., Tachikawa, N., Dokko, K., and Watanabe, M. (2012). Glyme-lithium salt equimolar molten mixtures: concentrated solutions or solvate ionic liquids? J. Phys. Chem. B *116*, 11323–11331.
13. Tamura, T., Hachida, T., Yoshida, K., Tachikawa, N., Dokko, K., and Watanabe, M. (2010). New glyme-cyclic imide lithium salt complexes as thermally stable electrolytes for lithium batteries. J. Power Sources *195*, 6095–6100.
14. Tamura, T., Yoshida, K., Hachida, T., Tsuchiya, M., Nakamura, M., Kazue, Y., Tachikawa, N., Dokko, K., and Watanabe, M. (2010). Physicochemical properties of Glyme-Li salt complexes as a new family of room-temperature ionic liquids. Chem. Lett. *39*, 753–755.
15. Yoshida, K., Nakamura, M., Kazue, Y., Tachikawa, N., Tsuzuki, S., Seki, S., Dokko, K., and Watanabe, M. (2011). Oxidative-stability enhancement and charge transport mechanism in Glyme-lithium salt equimolar complexes. J. Am. Chem. Soc. *133*, 13121–13129.
16. Yoshida, K., Tsuchiya, M., Tachikawa, N., Dokko, K., and Watanabe, M. (2011). Change from glyme solutions to quasi-ionic liquids for binary mixtures consisting of lithium bis(trifluoromethanesulfonyl)amide and glymes. J. Phys. Chem. C *115*, 18384–18394.

17. Henderson, W.A. (2006). Glyme–lithium salt phase behavior. J. Phys. Chem. B *110*, 13177–13183.

18. Choquette, Y., Brisard, G., Parent, M., Brouillette, D., Perron, G., Desnoyers, J.E., Armand, M., Gravel, D., and Slougui, N. (1998). Sulfamides and glymes as aprotic solvents for lithium batteries. J. Electrochem. Soc. *145*, 3500–3507.

19. Seki, S., Takei, K., Miyashiro, H., and Watanabe, M. (2011). Physicochemical and electrochemical properties of Glyme-$LiN(SO_2F)_2$ complex for safe lithium-ion secondary battery electrolyte. J. Electrochem. Soc. *158*, A769–A774.

20. Suo, L.M., Hu, Y.S., Li, H., Armand, M., and Chen, L.Q. (2013). A new class of Solvent-in-Salt electrolyte for high-energy rechargeable metallic lithium batteries. Nat. Commun. *4*, 1481.

21. Yamada, Y., Furukawa, K., Sodeyama, K., Kikuchi, K., Yaegashi, M., Tateyama, Y., and Yamada, A. (2014). Unusual stability of acetonitrile-based superconcentrated electrolytes for fast-charging lithium-ion batteries. J. Am. Chem. Soc. *136*, 5039–5046.

22. Wang, J., Yamada, Y., Sodeyama, K., Chiang, C.H., Tateyama, Y., and Yamada, A. (2016). Superconcentrated electrolytes for a high-voltage lithium-ion battery. Nat. Commun. *7*, 12032.

23. Shiga, T., Okuda, C.-a., Kato, Y., and Kondo, H. (2018). Highly concentrated electrolytes containing a phosphoric acid ester amide with self-extinguishing properties for use in lithium batteries. J. Phys. Chem. C *122*, 9738–9745.

24. Suo, L., Borodin, O., Gao, T., Olguin, M., Ho, J., Fan, X., Luo, C., Wang, C., and Xu, K. (2015). "Water-in-salt" electrolyte enables high-voltage aqueous lithium-ion chemistries. Science *350*, 938–943.

25. Yamada, Y., Usui, K., Sodeyama, K., Ko, S., Tateyama, Y., and Yamada, A. (2016). Hydrate-melt electrolytes for high-energy-density aqueous batteries. Nat. Energy *1*, 16129.

26. Suo, L., Borodin, O., Sun, W., Fan, X., Yang, C., Wang, F., Gao, T., Ma, Z., Schroeder, M., von Cresce, A., et al. (2016). Advanced high-voltage aqueous lithium-ion battery enabled by "water-in-Bisalt" electrolyte. Angew. Chem. Int. Ed. Engl. *55*, 7136–7141.

27. Suo, L., Borodin, O., Wang, Y., Rong, X., Sun, W., Fan, X., Xu, S., Schroeder, M.A., Cresce, A.V., Wang, F., et al. (2017). "Water-in-Salt" electrolyte makes aqueous sodium-ion battery safe, green, and long-lasting. Adv. Energy Mater. *7*, 1701189.

28. Wang, F., Borodin, O., Gao, T., Fan, X., Sun, W., Han, F., Faraone, A., Dura, J.A., Xu, K., and Wang, C. (2018). Highly reversible zinc metal anode for aqueous batteries. Nat. Mater. *17*, 543–549.

29. Yang, C., Suo, L., Borodin, O., Wang, F., Sun, W., Gao, T., Fan, X., Hou, S., Ma, Z., Amine, K., et al. (2017). Unique aqueous Li-ion/sulfur chemistry with high energy density and reversibility. Proc. Natl. Acad. Sci. USA *114*, 6197–6202.

30. Zhang, C., Holoubek, J., Wu, X., Daniyar, A., Zhu, L., Chen, C., Leonard, D.P., Rodríguez-Pérez, I.A., Jiang, J.X., Fang, C., et al. (2018). A $ZnCl_2$ water-in-salt electrolyte for a reversible Zn metal anode. Chem. Commun. (Camb.) *54*, 14097–14099.

31. Yang, C., Chen, J., Qing, T., Fan, X., Sun, W., von Cresce, A., Ding, M.S., Borodin, O., Vatamanu, J., Schroeder, M.A., et al. (2017). 4.0 V aqueous Li-Ion batteries. Joule *1*, 122–132.

32. Yang, C., Chen, J., Ji, X., Pollard, T.P., Lü, X., Sun, C.J., Hou, S., Liu, Q., Liu, C., Qing, T., et al. (2019). Aqueous Li-ion battery enabled by halogen conversion–intercalation chemistry in graphite. Nature *569*, 245–250.

33. Xu, K., and Wang, C. (2016). Batteries: widening voltage windows. Nat. Ener. *1*, 16161.

34. Chen, S., Zheng, J., Mei, D., Han, K.S., Engelhard, M.H., Zhao, W., Xu, W., Liu, J., and Zhang, J.G. (2018). High-voltage lithium-metal batteries enabled by localized high-concentration electrolytes. Adv. Mater. *30*, e1706102.

35. Yu, L., Chen, S., Lee, H., Zhang, L., Engelhard, M.H., Li, Q., Jiao, S., Liu, J., Xu, W., and Zhang, J.-G. (2018). A localized high-concentration electrolyte with optimized solvents and lithium difluoro(oxalate)borate additive for stable lithium metal batteries. ACS Energy Lett. *3*, 2059–2067.

36. Ren, X., Zou, L., Cao, X., Engelhard, M.H., Liu, W., Burton, S.D., Lee, H., Niu, C., Matthews, B.E., Zhu, Z., et al. (2019). Enabling high-voltage lithium-metal batteries under practical conditions. Joule *3*, 1662–1676.

37. Chen, S., Zheng, J., Yu, L., Ren, X., Engelhard, M.H., Niu, C., Lee, H., Xu, W., Xiao, J., Liu, J., and Zhang, J.-G. (2018). High-efficiency lithium metal batteries with fire-retardant electrolytes. Joule *2*, 1548–1558.

38. Ren, X., Chen, S., Lee, H., Mei, D., Engelhard, M.H., Burton, S.D., Zhao, W., Zheng, J., Li, Q., Ding, M.S., et al. (2018). Localized high-concentration sulfone electrolytes for high-efficiency lithium-metal batteries. Chem *4*, 1877–1892.

39. Huang, Q., Pollard, T.P., Ren, X., Kim, D., Magasinski, A., Borodin, O., and Yushin, G. (2019). Fading mechanisms and voltage hysteresis in FeF_2–NiF_2 solid solution cathodes for lithium and lithium-ion batteries. Small *15*, e1804670.

40. Alvarado, J., Schroeder, M.A., Pollard, T.P., Wang, X., Lee, J.Z., Zhang, M., Wynn, T., Ding, M., Borodin, O., Meng, Y.S., et al. (2019). Bisalt ether electrolytes: a pathway towards lithium metal batteries with Ni-rich cathodes. Energy Environ. Sci. *12*, 780–794.

41. Borodin, O. (2019). Challenges with prediction of battery electrolyte electrochemical stability window and guiding the electrode – electrolyte stabilization. Curr. Opin. Electrochem. *13*, 86–93.

42. Borodin, O., and Smith, G.D. (2006). LiTFSI structure and transport in ethylene carbonate from Molecular Dynamics simulations. J. Phys. Chem. B *110*, 4971–4977.

43. Xu, K. (2004). Nonaqueous liquid electrolytes for lithium-based rechargeable batteries. Chem. Rev. *104*, 4303–4417.

44. Bernal, J.D., and Fowler, R.H. (1933). A theory of water and ionic solution, with particular reference to hydrogen and hydroxyl ions. J. Chem. Phys. *1*, 515–548.

45. Seo, D.M., Borodin, O., Han, S.-D., Boyle, P.D., and Henderson, W.A. (2012). Electrolyte solvation and ionic Association II. Acetonitrile-lithium salt mixtures: highly dissociated salts. J. Electrochem. Soc. *159*, A1489–A1500.

46. Seo, D.M., Borodin, O., Han, S.-D., Ly, Q., Boyle, P.D., and Henderson, W.A. (2012). Electrolyte solvation and ionic association. J. Electrochem. *S159*, A553–A565.

47. Han, S.-D., Borodin, O., Seo, D.M., Zhou, Z.-B., and Henderson, W.A. (2014). Electrolyte solvation and ionic association: V. Acetonitrile-lithium bis(fluorosulfonyl)imide (LiFSI) mixtures. J. Electrochem. Soc. *161*, A2042–A2053.

48. Wan, C., Hu, M.Y., Borodin, O., Qian, J., Qin, Z., Zhang, J.-G., and Hu, J.Z. (2016). Natural abundance ^{17}O, ^{6}Li NMR and molecular modeling studies of the solvation structures of lithium bis(fluorosulfonyl)imide/1,2-dimethoxyethane liquid electrolytes. J. Power Sources *307*, 231–243.

49. Borodin, O., Suo, L., Gobet, M., Ren, X., Wang, F., Faraone, A., Peng, J., Olguin, M., Schroeder, M., Ding, M.S., and Xu, K. (2017). Liquid structure with nano-heterogeneity promotes cationic transport in concentrated electrolytes. ACS Nano *11*, 10462–10471.

50. Chapman, N., Borodin, O., Yoon, T., Nguyen, C.C., and Lucht, B.L. (2017). Spectroscopic and density functional theory characterization of common lithium salt solvates in carbonate electrolytes for lithium batteries. J. Phys. Chem. C *121*, 2135–2148.

51. Zhang, C., Ueno, K., Yamazaki, A., Yoshida, K., Moon, H., Mandai, T., Umebayashi, Y., Dokko, K., and Watanabe, M. (2014). Chelate effects in Glyme/Lithium bis(trifluoromethanesulfonyl)amide solvate ionic liquids. I. Stability of solvate cations and correlation with electrolyte properties. J. Phys. Chem. B *118*, 5144–5153.

52. McOwen, D.W., Seo, D.M., Borodin, O., Vatamanu, J., Boyle, P.D., and Henderson, W.A. (2014). Concentrated electrolytes: decrypting electrolyte properties and reassessing Al corrosion mechanisms. Energy Environ. Sci. *7*, 416–426.

53. Aihara, Y., Sugimoto, K., Price, W.S., and Hayamizu, K. (2000). Ionic conduction and self-diffusion near infinitesimal concentration in lithium salt-organic solvent electrolytes. J. Chem. Phys. *113*, 1981–1991.

54. Borodin, O., Henderson, W.A., Fox, E.T., Berman, M., Gobet, M., and Greenbaum, S. (2013). Influence of solvent on ion aggregation and transport in $PY_{15}TFSI$ ionic liquid–aprotic solvent mixtures. J. Phys. Chem. B *117*, 10581–10588.

55. Aihara, Y., Bando, T., Nakagawa, H., Yoshida, H., Hayamizu, K., Akiba, E., and Price, W.S. (2004). Ion transport properties of six lithium

salts dissolved in gamma-butyrolactone studied by self-diffusion and ionic conductivity measurements. J. Electrochem. Soc. *151*, A119–A122.

56. Chen, X., Hou, T.-Z., Li, B., Yan, C., Zhu, L., Guan, C., Cheng, X.-B., Peng, H.-J., Huang, J.-Q., and Zhang, Q. (2017). Towards stable lithium-sulfur batteries: mechanistic insights into electrolyte decomposition on lithium metal anode. Energy Storage Materials *8*, 194–201.

57. Allen, J.L., Borodin, O., Seo, D.M., and Henderson, W.A. (2014). Combined quantum chemical/Raman spectroscopic analyses of Li^+ cation solvation: cyclic carbonate solvents—ethylene carbonate and propylene carbonate. J. Power Sources *267*, 821–830.

58. von Wald Cresce, A., Gobet, M., Borodin, O., Peng, J., Russell, S.M., Wikner, E., Fu, A., Hu, L., Lee, H.-S., Zhang, Z., et al. (2015). Anion solvation in carbonate-based electrolytes. J. Phys. Chem. C *119*, 27255–27264.

59. von Wald Cresce, A., Borodin, O., and Xu, K. (2012). Correlating Li^+ solvation sheath structure with Interphasial chemistry on graphite. J. Phys. Chem. C *116*, 26111–26117.

60. Borodin, O., and Smith, G.D. (2007). Li^+ transport mechanism in oligo(ethylene oxide) s compared to carbonates. J. Solution Chem. *36*, 803–813.

61. Seo, D.M., Borodin, O., Balogh, D., O'Connell, M., Ly, Q., Han, S.-D., Passerini, S., and Henderson, W.A. (2013). Electrolyte solvation and ionic Association III. Acetonitrile-lithium salt mixtures–transport properties. J. Electrochem. Soc. *160*, A1061–A1070.

62. Forsyth, M., Yoon, H., Chen, F.F., Zhu, H.J., MacFarlane, D.R., Armand, M., and Howlett, P.C. (2016). Novel Na+ ion diffusion mechanism in mixed organic-inorganic ionic liquid electrolyte leading to high Na+ transference number and stable, high rate electrochemical cycling of sodium cells. J. Phys. Chem. C *120*, 4276–4286.

63. Hayamizu, K., Aihara, Y., Arai, S., and Martinez, C.G. (1999). Pulse-gradient spin-echo ^1H, ^7Li, and ^{19}F NMR diffusion and ionic conductivity measurements of 14 organic electrolytes containing $LiN(SO_2CF_3)_2$. J. Phys. Chem. B *103*, 519–524.

64. Borodin, O., Giffin, G.A., Moretti, A., Haskins, J.B., Lawson, J.W., Henderson, W.A., and Passerini, S. (2018). Insights into the structure and transport of the lithium, sodium, magnesium, and zinc bis(trifluoromethansulfonyl)imide salts in ionic liquids. J. Phys. Chem. C *122*, 20108–20121.

65. Dong, D., Sälzer, F., Roling, B., and Bedrov, D. (2018). How efficient is Li^+ ion transport in solvate ionic liquids under anion-blocking conditions in a battery? Phys. Chem. Chem. Phys. *20*, 29174–29183.

66. Liyana-Arachchi, T.P., Haskins, J.B., Burke, C.M., Diederichsen, K.M., McCloskey, B.D., and Lawson, J.W. (2018). Polarizable molecular dynamics and experiments of 1,2-dimethoxyethane electrolytes with lithium and sodium salts: structure and transport properties. J. Phys. Chem. B *122*, 8548–8559.

67. Dong, D., and Bedrov, D. (2018). Charge transport in [Li(tetraglyme)] [bis(trifluoromethane) sulfonimide] solvate ionic liquids: insight from molecular dynamics simulations. J. Phys. Chem. B *122*, 9994–10004.

68. Okoshi, M., Chou, C.P., and Nakai, H. (2018). Theoretical analysis of carrier ion diffusion in superconcentrated electrolyte solutions for sodium-ion batteries. J. Phys. Chem. B *122*, 2600–2609.

69. Borodin, O., and Smith, G.D. (2009). Quantum chemistry and Molecular Dynamics simulation study of dimethyl carbonate: ethylene carbonate electrolytes doped with $LiPF_6$. J. Phys. Chem. B *113*, 1763–1776.

70. Self, J., Fong, K.D., and Persson, K.A. (2019). Transport in superconcentrated $LiPF_6$ and $LiBF_4$/propylene carbonate electrolytes. ACS Energy Lett. *4*, 2843–2849.

71. Alvarado, J., Schroeder, M.A., Zhang, M., Borodin, O., Gobrogge, E., Olguin, M., Ding, M.S., Gobet, M., Greenbaum, S., Meng, Y.S., and Xu, K. (2018). A carbonate-free, sulfone-based electrolyte for high-voltage Li-ion batteries. Mater. Today *21*, 341–353.

72. Dokko, K., Watanabe, D., Ugata, Y., Thomas, M.L., Tsuzuki, S., Shinoda, W., Hashimoto, K., Ueno, K., Umebayashi, Y., and Watanabe, M. (2018). Direct evidence for Li ion hopping conduction in highly concentrated sulfolane-based liquid electrolytes. J. Phys. Chem. B *122*, 10736–10745.

73. Hayamizu, K. (2012). Temperature dependence of self-diffusion coefficients of ions and solvents in ethylene carbonate, propylene carbonate, and diethyl carbonate single solutions and ethylene carbonate + diethyl carbonate binary solutions of LiPF6 studied by NMR. J. Chem. Eng. Data *57*, 2012–2017.

74. Yang, Y., Davies, D.M., Yin, Y., Borodin, O., Lee, J.Z., Fang, C., Olguin, M., Zhang, Y., Sablina, E.S., Wang, X., et al. (2019). High-efficiency lithium-metal anode enabled by liquefied gas electrolytes. Joule *3*, 1986–2000.

75. Borodin, O., Han, S.-D., Daubert, J.S., Seo, D.M., Yun, S.-H., and Henderson, W.A. (2015). Electrolyte Solvation and Ionic Association: VI. Acetonitrile-lithium salt mixtures: highly associated salts revisited. J. Electrochem. Soc. *162*, A501–A510.

76. Wohde, F., Balabajew, M., and Roling, B. (2016). Li+ transference numbers in liquid electrolytes obtained by very-low-frequency impedance spectroscopy at variable electrode distances. J. Electrochem. Soc. *163*, A714–A721.

77. Suo, L., Oh, D., Lin, Y., Zhuo, Z., Borodin, O., Gao, T., Wang, F., Kushima, A., Wang, Z., Kim, H.C., et al. (2017). How solid-electrolyte interphase forms in aqueous electrolytes. J. Am. Chem. Soc. *139*, 18670–18680.

78. McEldrew, M., Goodwin, Z.A.H., Kornyshev, A.A., and Bazant, M.Z. (2018). Theory of the double layer in water-in-salt electrolytes. J. Phys. Chem. Lett. *9*, 5840–5846.

79. Vatamanu, J., and Borodin, O. (2017). Ramifications of water-in-salt interfacial structure at charged electrodes for electrolyte electrochemical stability. J. Phys. Chem. Lett. *8*, 4362–4367.

80. Borodin, O., Ren, X., Vatamanu, J., von Wald Cresce, A., Knap, J., and Xu, K. (2017). Modeling insight into battery electrolyte electrochemical stability and interfacial structure. Acc. Chem. Res. *50*, 2886–2894.

81. Vatamanu, J., Borodin, O., and Smith, G.D. (2012). Molecular dynamics simulation studies of the structure of a mixed carbonate/$LiPF_6$ electrolyte near graphite surface as a function of electrode potential. J. Phys. Chem. C *116*, 1114–1121.

82. Raberg, J.H., Vatamanu, J., Harris, S.J., van Oversteeg, C.H.M., Ramos, A., Borodin, O., and Cuk, T. (2019). Probing electric double-layer composition via in situ vibrational spectroscopy and molecular simulations. J. Phys. Chem. Lett. *10*, 3381–3389.

83. Kim, H., Wu, F., Lee, J.T., Nitta, N., Lin, H.-T., Oschatz, M., Cho, W.I., Kaskel, S., Borodin, O., and Yushin, G. (2015). In situ formation of protective coatings on sulfur cathodes in lithium batteries with LiFSI-based organic electrolytes. Adv. Energy Mater. *5*, 1401792.

84. Qian, J., Henderson, W.A., Xu, W., Bhattacharya, P., Engelhard, M., Borodin, O., and Zhang, J.G. (2015). High rate and stable cycling of lithium metal anode. Nat. Commun. *6*, 6362.

85. Azov, V.A., Egorova, K.S., Seitkalieva, M.M., Kashin, A.S., and Ananikov, V.P. (2018). "Solvent-in-salt" systems for design of new materials in chemistry, biology and energy research. Chem. Soc. Rev. *47*, 1250–1284.

86. Sodeyama, K., Yamada, Y., Aikawa, K., Yamada, A., and Tateyama, Y. (2014). Sacrificial anion reduction mechanism for electrochemical stability improvement in highly concentrated Li-salt electrolyte. J. Phys. Chem. C *118*, 14091–14097.

87. Yamada, Y., Usui, K., Chiang, C.H., Kikuchi, K., Furukawa, K., and Yamada, A. (2014). General observation of lithium intercalation into graphite in ethylene-carbonate-free superconcentrated electrolytes. ACS Appl. Mater. Interfaces *6*, 10892–10899.

88. Cresce, A.v., Russell, S.M., Baker, D.R., Gaskell, K.J., and Xu, K. (2014). In situ and quantitative characterization of solid electrolyte interphases. Nano Lett. *14*, 1405–1412.

89. Dubouis, N., Lemaire, P., Mirvaux, B., Salager, E., Deschamps, M., and Grimaud, A. (2018). The role of the hydrogen evolution reaction in the solid–electrolyte interphase formation mechanism for "water-in-Salt" electrolytes. Energy Environ. Sci. *11*, 3491–3499.

90. Lee, M.H., Kim, S.J., Chang, D., Kim, J., Moon, S., Oh, K., Park, K.-Y., Seong, W.M., Park, H., Kwon, G., et al. (2019). Toward a low-cost high-voltage sodium aqueous rechargeable battery. Mater. Today *29*, 26–36.

91. Zheng, J., Tan, G., Shan, P., Liu, T., Hu, J., Feng, Y., Yang, L., Zhang, M., Chen, Z., Lin, Y., et al. (2018). Understanding thermodynamic and kinetic contributions in expanding the stability window of aqueous electrolytes. Chem *4*, 2872–2882.

92. Guha, A., Narayanaru, S., and Narayanan, T.N. (2018). Tuning the hydrogen evolution reaction on metals by lithium salt. ACS Appl. Energy Mater. *1*, 7116–7122.

93. Huang, Q., and Lyons, T.W. (2018). Electrodeposition of rhenium with suppressed hydrogen evolution from water-in-salt electrolyte. Electrochem. Commun. *93*, 53–56.

94. Huang, Q., and Hu, Y. (2018). Electrodeposition of superconducting rhenium with water-in-salt electrolyte. J. Electrochem. Soc. *165*, D796–D801.

95. Winter, M., Barnett, B., and Xu, K. (2018). Before Li ion batteries. Chem. Rev. *118*, 11433–11456.

96. Yamada, Y., Takazawa, Y., Miyazaki, K., and Abe, T. (2010). Electrochemical lithium intercalation into graphite in dimethyl sulfoxide-based electrolytes: effect of solvation structure of lithium ion. J. Phys. Chem. C *114*, 11680–11685.

97. Yang, C., Ji, X., Fan, X., Gao, T., Suo, L., Wang, F., Sun, W., Chen, J., Chen, L., Han, F., et al. (2017). Flexible aqueous Li-Ion battery with high energy and power densities. Adv. Mater. Weinheim *29*, 29034519.

98. Wang, F., Borodin, O., Ding, M.S., Gobet, M., Vatamanu, J., Fan, X., Gao, T., Eidson, N., Liang, Y., Sun, W., et al. (2018). Hybrid aqueous/non-aqueous electrolyte for safe and high-energy Li-Ion batteries. Joule *2*, 927–937.

99. Takada, K., Yamada, Y., Watanabe, E., Wang, J., Sodeyama, K., Tateyama, Y., Hirata, K., Kawase, T., and Yamada, A. (2017). Unusual passivation ability of superconcentrated electrolytes toward hard carbon negative electrodes in sodium-ion batteries. ACS Appl. Mater. Interfaces *9*, 33802–33809.

100. Nakanishi, A., Ueno, K., Watanabe, D., Ugata, Y., Matsumae, Y., Liu, J., Thomas, M.L., Dokko, K., and Watanabe, M. (2019). Sulfolane-based highly concentrated electrolytes of lithium bis(trifluoromethanesulfonyl)amide: ionic transport, Li-Ion coordination, and Li–S battery performance. J. Phys. Chem. C *123*, 14229–14238.

101. Lee, C.W., Pang, Q., Ha, S., Cheng, L., Han, S.D., Zavadil, K.R., Gallagher, K.G., Nazar, L.F., and Balasubramanian, M. (2017). Directing the lithium–sulfur reaction pathway via sparingly solvating electrolytes for high energy density batteries. ACS Cent. Sci. *3*, 605–613.

102. Wu, F., and Yu, Y. (2018). Toward true lithium-air batteries. Joule *2*, 815–817.

103. Dong, Q., Yao, X., Zhao, Y., Qi, M., Zhang, X., Sun, H., He, Y., and Wang, D. (2018). Cathodically stable Li-O_2 battery operations using water-in-salt electrolyte. Chem *4*, 1345–1358.

104. Son, S.B., Gao, T., Harvey, S.P., Steirer, K.X., Stokes, A., Norman, A., Wang, C., Cresce, A., Xu, K., and Ban, C. (2018). An artificial interphase enables reversible magnesium chemistry in carbonate electrolytes. Nat. Chem. *10*, 532–539.

105. Wang, F., Fan, X., Gao, T., Sun, W., Ma, Z., Yang, C., Han, F., Xu, K., and Wang, C. (2017). High-voltage aqueous magnesium ion batteries. ACS Cent. Sci. *3*, 1121–1128.

106. Xu, W., Wang, J.L., Ding, F., Chen, X.L., Nasybulin, E., Zhang, Y.H., and Zhang, J.G. (2014). Lithium metal anodes for rechargeable batteries. Energy Environ. Sci. *7*, 513–537.

107. Liu, K., Kong, B., Liu, W., Sun, Y., Song, M.-S., Chen, J., Liu, Y., Lin, D., Pei, A., and Cui, Y. (2018). Stretchable lithium metal anode with improved mechanical and electrochemical cycling stability. Joule *2*, 1857–1865.

108. Fang, C., Li, J., Zhang, M., Zhang, Y., Yang, F., Lee, J.Z., Lee, M.H., Alvarado, J., Schroeder, M.A., Yang, Y., et al. (2019). Quantifying inactive lithium in lithium metal batteries. Nature *572*, 511–515.

109. Fan, X., Chen, L., Borodin, O., Ji, X., Chen, J., Hou, S., Deng, T., Zheng, J., Yang, C., Liou, S.C., et al. (2018). Non-flammable electrolyte enables Li-metal batteries with aggressive cathode chemistries. Nat. Nanotechnol. *13*, 715–722.

110. Wang, C.S., Meng, Y.S., and Xu, K. (2018). Fluorinating interphases. J. Electrochem. Soc. *166*, A5184–A5186.

111. Cao, X., Ren, X., Zou, L., Engelhard, M.H., Huang, W., Wang, H., Matthews, B.E., Lee, H., Niu, C., Arey, B.W., et al. (2019). Monolithic solid–electrolyte interphases formed in fluorinated orthoformate-based electrolytes minimize Li depletion and pulverization. Nat. Energy *4*, 796–805.

112. Fan, X., Ji, X., Han, F., Yue, J., Chen, J., Chen, L., Deng, T., Jiang, J., and Wang, C. (2018). Fluorinated solid electrolyte interphase enables highly reversible solid-state Li metal battery. Sci. Adv. *4*, eaau9245.

113. Fan, X., Ji, X., Chen, L., Chen, J., Deng, T., Han, F., Yue, J., Piao, N., Wang, R., Zhou, X., et al. (2019). All-temperature batteries enabled by fluorinated electrolytes with non-polar solvents. Nat. Energy *4*, 882–890.